学位論文

Histological and Molecular Basis of Macaque Sexual Skin

（マカク性皮の組織学と分子基盤）

平成 27 年 11 月 博士（理学） 申請

東京大学大学院理学系研究科

生物科学専攻

小野　英理

Doctoral Thesis

Histological and Molecular Basis of Macaque Sexual Skin

Eiri Ono

Department of Biological Sciences

Graduate School of Science

The University of Tokyo

2015

Abstract

Females of some catarrhine species develop conspicuous sexual skin transformation in their faces and hindlimbs/hindquarters. This “sexual skin” is thought to be tightly involved in socio-sexual signaling. Changes in the sexual skin are simply referred to as swelling and coloration. The graded-signals hypothesis by Nunn (1999) suggests that exaggerated swelling of sexual skin may represent the probability of ovulation in a multimale–multifemale social structure. Graded changes in sexual skin size allow females to benefit mate guarding from dominant males at peak swelling and also to mate with subordinate males outside peak swelling, which results in paternity confusion and a reduced risk of infanticide. The hypothesis is suitable for species where most adult females show exaggerated swelling, such as chimpanzees and baboons, but is not suitable for species where adolescent females show the swelling, such as Japanese macaques. In contrast, the function of coloration relating to cue for ovulation comprises several facets, because the coloration mechanism remains unsolved. To elucidate the function of sexual skin coloration in breeding behavior, it is important to investigate the influence of sex hormones on the coloration.

Among the genus *Macaca* (one of the radiated and adapted catarrhine groups with diverse sexual skin transformations), phylogenetically-related species such as the Japanese macaques (*Macaca fuscata*) and rhesus macaques (*Macaca mulatta*) have been reported to exhibit similar sexual skin characteristics. However, species similarities and differences in the coloration and swelling are empirically observed, and

they have not been examined. In the current study, sexual skin transformations, including coloration and swelling, were objectively measured via spectrocolorimetry and homology image analyses. Additionally, cutaneous factors, such as vascular capillaries, melanin granules, and hyaluronan were histologically examined in regard to the hormonal regulations. All of these variables can cause transformation of the sexual skin.

Spectrocolorimetry revealed that both macaque species exhibited similar seasonal coloration in their hindquarters. Compared with the non-mating season (NMS), the sexual skin became redder, darker, and yellower in the mating season (MS). The coloration was commonly modified by vasodilation in the macaques, which may be mediated by vascular pericytes expressing estrogen receptor alpha (ERα). In contrast, the two macaque species have differences in coloration and the mechanisms; the sexual skin of Japanese macaques is redder and darker than that of rhesus macaques. Vascularization and abundant melanin were found only in the Japanese macaques, which made their sexual skin redder and darker. Additionally, the sexual skin of rhesus macaques was affected by an increase in hyaluronan (HA) level leading to sexual swelling, which resulted in a loss of redness and darkness in sexual skin. These different bases of coloration result in seasonal variation in sexual skin color in different species.

As for hormonal regulation of these cutaneous factors, the localization of estrogen receptors (ERα and ERβ) and progesterone receptors (PR) were qualitatively same in both species. Seasonal analyses of ERα suggested that seasonal vasodilation and HA synthesis were mediated by pericytes and fibroblasts expressing ERα. The

vascularization, abundance of melanin, and an increased HA level are suggested to be long-term factors in skin coloration compared with vasodilation, which easily fluctuates by internal hormone levels, even in NMS. Therefore, sexual skin coloration may be mediated through long- and short-term cutaneous factors, which may generate robust signals for sexual skin coloration. Future studies using cultured vascular-related cells will allow further insights into the hormonal regulation of sexual skin coloration. The major mechanisms observed in this study will help to understand the effect of sexual skin on breeding behavior in primates. Species comparisons of these mechanisms will provide an insight into the sexual skin evolution in primates.

Contents

Chapter 1 General Introduction

Human females do not exhibit the timing of ovulation, which is "concealed ovulation." The concealed ovulation has been acquired through the human evolution. "Sexual skin," which is found in the females of some catarrhines, develops conspicuous transformation around the perineal skin of their hindlimbs/hindquarter [Collings, 1926; Dixson, 1983; Anderson and Bielert, 1994; Nunn, 1999; Higham et al., 2010]. This "sexual skin" is thought to be attractive for males and be tightly involved in socio-sexual signaling [Wickler, 1967; Gerald et al., 2007; Bradley and Mundy, 2008]. Changes in the sexual skin are simply referred to as swelling and coloration. Exaggerated swellings in the hindquarters are typical for females of the species where there is a multimale–multifemale and promiscuous social structure [Nunn, 1999]. As the swelling reaches its maximum size around the fertile period including the timing of ovulation in baboons [Higham et al., 2008], mandrills [Setchell and Wickings, 2004], chimpanzees [Deschner et al., 2004], and crested macaques [Higham et al., 2012], sexual skin swelling is believed to indicate likelihood of female fertility but does not pinpoint the timing of ovulation. The swelling occurs as graded signals, and it has been hypothesized that exaggerated swellings allow females to control male behavior by balancing the costs and benefits of mate guarding in multimale–multifemale social structure, so that dominant males tend to guard only at maximum swelling times, whereas females can copulate with multiple males outside the maximum swelling time to confuse paternity resulting in a reduced risk of infanticide; this is the "graded-signals

hypothesis" [Nunn, 1999].

The graded-signals hypothesis is a good explanation for species where most adult females show exaggerated swelling, such as in chimpanzees and some baboons. However, it is not suitable for species where adolescent females show greater swelling than adult females do, such as in rhesus macaques (*Macaca mulatta*), Japanese macaques (*Macaca fuscata*), and long-tailed macaques (*Macaca fascicularis*) [Anderson & Bielert, 1994]. If sexual swelling is the only component that has a role in paternity confusion, the effect of confusion tends to be weak in those macaques that form multimale–multifemale groups.

It has been reported that sexual swelling is not the only cue for female ovulation in Barbary macaques [Young et al., 2013], and it has been implied that the existence of synergy between further hormonal cues, such as coloration/reddening, and sexual swelling. However, in the previous reports, sexual skin coloration comprises several facets in the context of fertility and mating behavior in primates [Waitt et al., 2006; Higham et al., 2008; Wallner et al., 2011]. Some studies have reported that the hindquarter coloration is not accurate with respect to the fertile period [anubis baboon by Higham et al., 2008; rhesus macaques by Dubuc et al., 2009]. In contrast, in Japanese macaques, bright coloration of the hindquarter might contain meaningful physiological information [Wallner et al., 2011]. Additionally, it has been empirically observed that sexual skin of Japanese macaques swells less obviously and is much redder than that of the rhesus macaques [observed by J. Suzuki]. It is possible that female Japanese macaques use sexual skin coloration as cues for fertile periods rather

than swelling, although Japanese and rhesus macaques have been reported to show similar sexual skin characteristics.

Japanese macaques (*M. fuscata*) and rhesus macaques (*M. mulatta*) belong to the *fascicularis* lineage in the genus *Macaca* [Thierry, 2010]. The genus *Macaca* comprises more than 20 species, which have radiated and adapted to various environments [reviewed in Thierry, 2010; table 1.1]. Changes in the sexual skin are also diverse among these. Japanese macaques live in various environments ranging from warm to cool temperate zones in Japan, whereas rhesus macaques inhabit various environments of mainland Asia, such as India, China, and Southeast Asia. These two macaques share similar reproductive features [reviewed in Thierry, 2010]. For example, ovarian cycle length (Japanese macaques: 26.5 days; rhesus macaques: 28.3 days), the multimale–multifemale social structure, multi-mounting behavior, and seasonal breeding are all similar, although age at first birth is delayed in the Japanese macaques (Japanese macaques: 5 years; rhesus macaques: 4 years). Sexual swellings have been recognized in adolescent females of both species [Anderson and Bielert, 1994]. However, similarities and differences in sexual skin coloration between the Japanese and rhesus macaques have not been quantitatively analyzed; these backgrounds prompted me to examine and compare sexual skin coloration and its mechanism between the two macaque species.

There is a consensus that sex steroid hormones mediate sexual skin transformation [Czaja et al., 1977; Domb and Pagel 2001; Wallner et al., 2011]. A simple model was suggested where estrogen prompts sexual skin to swell, whereas

progesterone restores during the menstrual cycle in ovariectomized pig-tailed macaques (*M. nemestrina*) [Carlisle, et al., 1981]. It is important to note that there must be cutaneous factors near skin surface that are regulated by sex hormones and affect sexual skin coloration. It is known that various factors affect skin coloration in humans [Jablonski and Chaplin, 2000; Jablonski, 2004]. Of these factors, melanin pigments and vascular capillaries including hemoglobin are major factors [Alaluf et al., 2002a; Changizi et al., 2006]. However, which cutaneous factors, including pigments, can affect sexual skin coloration through hormonal regulation are yet to be investigated. To reveal the common mechanisms of skin coloration relating to sex hormones in closely related macaques, relationships between skin color and the local condition of skin tissue were seasonally compared between NMS, as the period without hormonal surges, and MS, as the period with cyclic hormonal surges. Examining factor(s) of sexual skin coloration and the hormonal regulation helps to understand the role(s) of coloration on breeding behavior in the macaques.

Table 1.1

Sexual swelling and copulation patterns in macaques

	SPECIES	SWELLING	SOCIAL SYSTEM (Single/Multi male)	SEASONAL BREEDING (Yes/No)
Fascicularis lineage	*Macaca fascicularis*	Adolescence*1	M	N
	M. mulatta	Adolescence	M	Y
	M. fuscata	Adolescence	M	Y
	M. cyclopis	Adolescence	M	Y
Sinica-arctoides lineage	*M. sinica*	None	M	Y
	M. radiata	None	M	Y
	M. assamensis	Adolescence	M	N
	M. thibetana	None	M	Y
	M. arctoides	None	M	N
Silenus-sylvanus lineage	*M. silenus*	Large	M	N
	M. sylvanus	Large	M	Y
	M. maurus	Large	M	N
	M. nemestrina	Large	M	N
	M. nigra	Large	M	N
	M. tonkeana	Large	M	N

*1 Swelling occurs in adolescent females only.

[Modified from Nunn, 1999 and a review by Thierry, 2010]

Chapter 2 Seasonal changes in sexual skin color

2.1 Introduction

Species differences in sexual skin coloration between Japanese and rhesus macaques have only been observed empirically and have not been quantitatively analyzed. There are some appropriate methods for measurement of skin color. Visual observation, digital photography, and spectrocolorimetry have all been used for skin color measurement [Stevens et al., 2009]. Among these, spectrocolorimetry, which obtains direct color data, is applicable to reared animals and the obtained color data are objective without interferences such as stray light. For the evaluation of the obtained color data, there are two major protocols. A model of common color space, such as the CIELAB space was developed for human color vision and a Receptor-Noise Limited (RNL) model [Vorobyev and Osorio, 1998] that uses species-specific data on the peripheral visual system, can be used. Data for the species-specific visual system are not available for the Japanese macaques yet but were obtained for the rhesus macaques [Bowmaker et al., 1978]. The CIELAB space can provide great insights into the relationship between skin color and pigmentation, such as measurement of melanin and hemoglobin, in humans [Weatherall and Coombs, 1992; Zonios et al., 2001; Alaluf et al., 2002a; Stephen et al., 2009]. Furthermore, it was shown that in mandrills (*Mandrillus sphinx*), a member of the papionines, the CIELAB model gave qualitatively similar results to those of the RNL model [Renoult et al., 2011]. The CIELAB model is thus considered as a useful tool to compare skin color in the catarrhines, who have a

uniform color vision system, which is similar to that of humans [Jacobs and Deegan, 1999; Changizi et al., 2006].

In this chapter, I aimed to evaluate and distinguish sexual skin coloration objectively in closely related macaques categorized into the *fascicularis* group, and to provide insights for factors associated with sexual skin coloration. I thus obtained color profiles of sexual skin from Japanese macaques and rhesus macaques using a spectrocolorimeter, and analyzed these in the CIELAB space.

2.2 Materials and Methods

2.2.1 Subjects

Twelve female Japanese macaques (*Macaca fuscata*: denoted by Mf in this thesis) aged 4–6 years, and 13 female rhesus macaques (*M. mulatta*: denoted by Mm) aged from 3–5 years were recruited for seasonal color measurement (table 2.1). All subjects in this thesis were reared at the Primate Research Institute, Kyoto University, Inuyama, Aichi, Japan. When I started the data collection in the non-mating season, reddening and swelling of sexual skin of the subjects were not recognized. I measured their color profiles in July (non-mating season: NMS) and October (mating season: MS) 2010, or in August (NMS) and November (MS) 2011. Two of 12 Japanese macaques were studied in 2010 and the other 10 in 2011, while six of 13 rhesus macaques were in 2010 and the other seven in 2011. This study followed the Guidelines for Care and Use

of non-Human Primates, Primate Research Institute, Kyoto University, and was approved by the Ethics committee of animal experiments of the institute.

2.2.2 Color measurements

To measure sexual skin coloration, one spot was selected 2–3 cm below the ischial callosity of each side (two spots for each subject in one season, figure 2.1). Prior to measurement, the subjects were anesthetized with ketamine hydrochloride (50 mg/mL Ketalar®, Sankyo-Parke-Davis & Co., Inc., Japan, 2.5 mg/kg) and medetomidine hydrochloride (Domitor® Meiji Seika Kaisha, Ltd. Tokyo, Japan, 0.1 mg/kg), and then the measurement spots were cleaned and shaved. The selected spots were measured in July (NMS) and October (MS) 2010 and in August (NMS) and November (MS) 2011. A single color measurement for each spot was conducted with a MINOLTA Spectrocolorimeter CG-411C (for the CIE D65/10° illuminant/observer condition). Three variables in the CIELAB color system, L^*, a^*, and b^*, were extracted for each measurement. The average values of L^*, a^* and b^* for each subject were calculated. The variables L^*, a^* and b^*, represent positions on the light–dark, red/magenta–green, and yellow–blue axis, respectively. The L^* ranges from 100 to 0, whereas the a^* and b^* values can take any figure theoretically, ranging from about 100 to −100 in general. To combine color data with histological analyses in the later chapters, biopsy was performed using a scalpel after the color measurement (see Chapter 3). Antidote to medetomidine, atipamezole hydrochloride (Domitor® Meiji Seika Kaisha, Ltd. Tokyo, Japan, 0.5 mg/kg), was administered to enable fully recovery

after the measurement and biopsy.

2.2.3 Data analysis

The data in July 2010 and August 2011 were combined for NMS, whereas the data in October 2010 and November 2011 were combined for MS. Changes in sex skin coloration between NMS and MS were analyzed using the paired t-test. The differences between the two species in each season were tested with the two-sample t-test and Welch's two-sample t-test, if necessary. The relationship between the seasonal differences (MS–NMS) in L^* and a^* was analyzed using linear regression. A p value less than 0.05 ($p < 0.05$) was considered statistically significant. Statistical analyses were performed using RStudio version 0.99.441 2009–2015 (RStudio, Inc. with R version 3.2.0 and ggplot2 package version 1.0.1, 2013, Hadley Wickham).

2.3 Results

Sexual skin coloration in 12 Japanese macaques and 13 rhesus macaques during NMS and MS is described in table 2.2 and visualized in figure 2.2 with the L^*, a^*, and b^* variables. In the Japanese macaques, the average ± SD of L^*, a^*, and b^* was 53.61 ± 3.31, 11.51 ± 4.57, and 6.66 ± 2.25, respectively, in NMS, and 46.60 ± 2.78, 19.97 ± 2.99, and 8.80 ± 1.34, respectively in MS. In the rhesus macaques, the average of L^*, a^*, b^* was 60.09 ± 3.96, 5.99 ± 4.59, and 5.83 ± 2.37, respectively, in NMS, and

52.70 ± 6.54, 13.62 ± 6.86, and 8.07 ± 1.43, respectively, in MS. During MS, decreases in L^* and increases in a^* and b^* were consistently observed in each subject for both the Japanese and rhesus macaques (table 2.2).

Differences in sexual skin coloration by species and season are also represented in figure 2.2. In both seasons, there were significant species differences observed for variable L^* (NMS: $t = -4.22$, $df = 23$, $p < 0.001$ by two-sample t-test; MS: $t = -3.08$, $df = 16.46$, $p < 0.01$ by Welch's two-sample t-test), and the variable a^* (NMS: $t = 3.01$, $df = 23$, $p < 0.01$ by two-sample t-test; MS: $t = 3.04$, $df = 16.68$, $p < 0.01$ by Welch's two sample t-test), but not for variable b^* (NMS: $t = 0.89$, $df = 23$, $p > 0.05$ by two-sample t-test; MS: $t = 1.31$, $df = 23$, $p > 0.05$ by two-sample t-test). In both species, the significant seasonal differences were observed for the variable L^* (Japanese macaques: $t = 6.55$, $df = 11$, $p < 0.001$ by paired t-test; rhesus macaques: $t = 6.48$, $df = 12$, $p < 0.001$ by paired t-test), the variable a^* (Japanese macaques: $t = -6.20$, $df = 11$, $p < 0.001$ by paired t-test; rhesus macaques: $t = -8.41$, $df = 12$, $p < 0.001$ by paired t-test), and the variable b^* (Japanese macaques: $t = -3.58$, $df = 11$, $p < 0.01$ by paired t-test; rhesus macaques: $t = -3.76$, $df = 12$, $p < 0.01$ by paired t-test).

The correlation coefficient between the seasonal differences in L^* and a^* was −0.94 ($r^2 = 0.89$, $t = -9.99$, $df = 13$, $p < 0.001$) in the Japanese macaques and −0.82 ($r^2 = 0.67$, $t = -6.56$, $df = 13$, $p < 0.001$) in the rhesus macaques.

2.4 Discussion

Sexual skin coloration of female Japanese macaques and rhesus macaques was spectrocolorimetrically measured and represented in the CIELAB space where sexual skin coloration could be biologically interpreted (table 2.2 and figure 2.2). I analyzed the obtained color values from two aspects: seasonal change and species difference. Seasonal changes in the sexual skin coloration in the Japanese macaques and rhesus macaques were more or less similar, i.e., sexual skin became darker, redder, and yellower in MS compared with that in NMS in both species. In detail, I also found that sexual skin of Japanese macaques was much redder (larger a^*) and darker (smaller L^*) than that of rhesus macaques through NMS and MS (figure 2.2). These observations are consistent with general observations that sexual skin of Japanese macaques appears to be redder than that of rhesus macaques. In terms of CIELAB values, similar dynamic changes in L^*, a^*, and b^* were observed, and it is thus conceivable that all color values in NMS as well as in MS in both macaques are under the control of the same factor(s). The sexual skin color in NMS is considered to represent the basic conditions without the surge of reproductive hormones, such as estrogen and progesterone [Nozaki et al., 1995]. Since the variables L^* and a^* but not b^* were significantly different between the two species in NMS (figure 2.2), it is suggested that the presence of different basic conditions that give lighter sexual skin to the rhesus macaques and redder sexual skin to the Japanese macaques. Thus, I demonstrated that the closely related these macaque species have similar but distinct sexual skin coloration.

Of the various factors modifying skin coloration, two major pigments—melanin and hemoglobin, are of particular interest. Melanin content modifies all three color values, in particular, L^* [Takiwaki, 1998; Alaluf et al., 2002b]. In human skin coloration, changes in L^* are mainly due to epidermal melanin content [Alaluf et al., 2002b] that is negatively correlated with L^* among humans [Alaluf et al., 2002a]. It is possible that the seasonal decrease in L^* in the Japanese and rhesus macaques is attributed to an increase in dermal melanin content. The lower L^* values in the Japanese macaques both in NMS and MS indicate a higher dermal melanin content in the Japanese macaques. Melanin production is induced by ultra-violet (UV) light in human [Pathak et al., 1962; Jablonski and Chaplin, 2000; Jablonski and Chaplin, 2010] and epidermal melanin content is subject to adaptive responses to UV light intensity. However, 17ß-estradiol (E2) also stimulates melanocyte tyrosinase activity in human skin [Ranson et al., 1988; McLeod et al., 1994]. Thus, I cannot rule out possible contributions from other factor(s) to melanization, and effects of E2 on dermal melanin content in macaques should be elucidated to explain the consistently lower L^* in the Japanese macaques.

The a^* variable represents the red-green color axis and higher a^* values were observed in the Japanese macaques in NMS and MS. In humans, red color of skin is mainly due to the superficial vascular plexus in the upper dermis [Takiwaki, 1998; Alaluf et al., 2002b] where reproductive hormones also play certain roles, such as improved vascularization by estrogens [Thornton, 2002]. As reproductive hormones can modulate blood vessels in the sexual skin in MS [Czaja et al., 1977], the increases in a^*

in MS may be due to vascularization and/or vasodilatation in Japanese and rhesus macaques. Consistently lower melanin contents in rhesus macaques were indicated by their higher L^* values both in NMS and MS. This may correspond to the observation by Montagna et al. (1964) that rhesus macaques have little melanin in the epidermis. Furthermore, the prediction by Collings (1926) that sexual skin reddening is not due to the pigmentation but due to the dynamics of sub-epidermal blood vessels also agrees with my data. I conclude that melanin contents support the baseline value of a^*, whereas the increased a^* in MS is due to blood hemoglobin in both species. The seasonal differences in L^* and a^* were highly correlated in both species (figure 2.3). The high correlation indicates L^* and a^* are influenced by the same factor(s) to change, namely, melanin and blood hemoglobin. The r^2 of regression line in the rhesus macaques was lower than that in the Japanese macaques. It indicates other factor(s) of coloration in the rhesus macaques, for example, sexual swelling. The structural change of sexual skin may also modify the coloration. Factors that can modify sexual skin coloration are discussed in Chapters 3 and 4.

It has been reported that adolescent females of both Japanese and rhesus macaques exhibit sexual swellings [Anderson and Bielert, 1994]. However, in this study, no Japanese macaques aged between 4–6 years exhibited sexual swelling, whereas 11 of the 13 rhesus macaques aged between 3–5 years did exhibit swelling. If the sexual skin coloration and swelling play a role in socio-sexual signaling, possible compensation for their bright red coloration may consequent in lack of sexual swelling and this should be taken into consideration; it has been reported that hindlimb bright coloration might

contain meaningful physiological information in Japanese macaques [Wallner et al., 2011].

For the analyses of spectrocolorimetric data of mandrills, the RNL model provided similar results as the CIELAB model [Renoult et al., 2011]. Preliminary data from the RNL model were also analyzed, which were consistent with those in the CIELAB model (data not shown) but the CIELAB model provided higher resolutions. The CIELAB model is suitable for such coloration studies. However, the RNL model that is based on the species-specific visual system may have the potential to understand cognitive consequences in the receiver of color signals. In conclusion, the study in this chapter has assessed objective and quantitative color measurements of sexual skin coloration and demonstrated similar and dissimilar profiles in the two closely related species. More detailed histological and molecular studies for the sexual skin in these macaque species will provide evolutionary insights into the mechanism of sexual skin development in primates. Spectrocolorimetry is a useful tool in conducting further research on species-specific, sex-specific, and age-related colorations in various parts of the body, particularly bare skin, among primates.

Table 2.1

Detailed information for the subjects recruited in this study.

ID	SAMPLING AGE (year)	SAMPLING YEAR	REARING CONDITION NMS	REARING CONDITION MS
M. fuscata				
2077	5	2010	Outdoor group cage*1	Outdoor enclosure*2
2111	4	2010	Outdoor group cage	Outdoor enclosure
2099	6	2011	Indoor individual cage*3	Indoor individual cage
2115	5	2011	Indoor individual cage	Indoor individual cage
2120	5	2011	Indoor individual cage	Indoor individual cage
2121	5	2011	Indoor individual cage	Indoor individual cage
2142	5	2011	Indoor individual cage	Indoor individual cage
2152	5	2011	Indoor individual cage	Indoor individual cage
2165	4	2011	Indoor individual cage	Indoor individual cage
2178	4	2011	Indoor individual cage	Indoor individual cage
2189	4	2011	Indoor individual cage	Indoor individual cage
2191	4	2011	Indoor individual cage	Indoor individual cage
M. mulatta				
1798	3	2010	Indoor individual cage	Outdoor group cage
1800	3	2010	Indoor individual cage	Outdoor group cage
1801	3	2010	Indoor individual cage	Outdoor group cage
1804	3	2010	Indoor individual cage	Outdoor group cage
1807	3	2010	Indoor individual cage	Outdoor group cage
1816	3	2010	Indoor individual cage	Outdoor group cage
1752	5	2011	Indoor individual cage	Indoor individual cage
1789	4	2011	Outdoor group cage	Indoor individual cage
1792	4	2011	Outdoor group cage	Indoor individual cage
1795	4	2011	Outdoor group cage	Indoor individual cage
1843	3	2011	Outdoor group cage	Outdoor group cage
1846	3	2011	Outdoor group cage	Outdoor group cage
1852	3	2011	Outdoor group cage	Outdoor group cage

NMS: non-mating season (July 2010 or August 2011); MS: mating season (October 2010 or November 2011).

*1 One or two males and three to six females

*2 Multiple males and females

*3 The photoperiod and humidity were not controlled, whereas the temperature was semi-controlled (about 15–30 °C) according to the seasons

Table 2.2

Sexual skin color of the Japanese and rhesus macaques represented by *L**, *a**, and *b** variables.

SPECIES	ID	NMS			MS		
		*L**	*a**	*b**	*L**	*a**	*b**
Mf	2077	53.31	9.21	5.64	51.56	12.67	8.63
	2111	51.08	10.39	3.72	45.38	18.92	7.39
	2099	55.39	15.45	9.88	49.79	20.33	8.78
	2115	55.79	10.45	6.49	49.13	17.53	5.66
	2120	52.50	17.49	8.63	47.39	22.92	9.18
	2121	55.23	5.23	4.13	43.25	20.55	8.18
	2142	57.08	10.85	7.50	49.26	18.31	8.97
	2152	49.27	19.55	9.42	45.93	23.68	9.77
	2165	50.89	13.30	6.31	44.51	19.33	9.43
	2178	48.00	12.50	8.05	43.32	20.90	10.85
	2189	55.99	9.92	7.30	45.67	21.56	10.16
	2191	58.79	3.82	2.84	43.99	22.94	8.62
Mm	1798	64.47	2.43	6.44	58.94	4.87	6.13
	1800	61.29	4.04	8.40	58.95	8.93	9.28
	1801	62.14	0.72	6.35	53.34	9.41	8.91
	1804	67.56	-1.29	-0.13	54.76	7.24	6.88
	1807	58.88	5.95	6.72	49.26	15.62	7.03
	1816	62.62	1.43	3.76	62.44	4.39	8.10
	1752	61.40	5.37	5.24	59.79	10.14	8.29
	1789	61.49	7.05	6.84	56.83	13.34	9.38
	1792	54.53	13.85	8.90	45.49	22.85	8.10
	1795	60.21	5.75	5.43	51.72	15.78	8.64
	1843	54.51	11.70	7.64	42.61	25.30	11.08
	1846	55.26	10.36	3.63	45.38	17.52	6.11
	1852	56.87	10.48	6.61	45.69	21.71	7.01

Mf: Japanese macaque; Mm: rhesus macaque; NMS: non-mating season (July, 2010 and Aug, 2011); MS: mating season (October, 2010 and November, 2011)

(A)

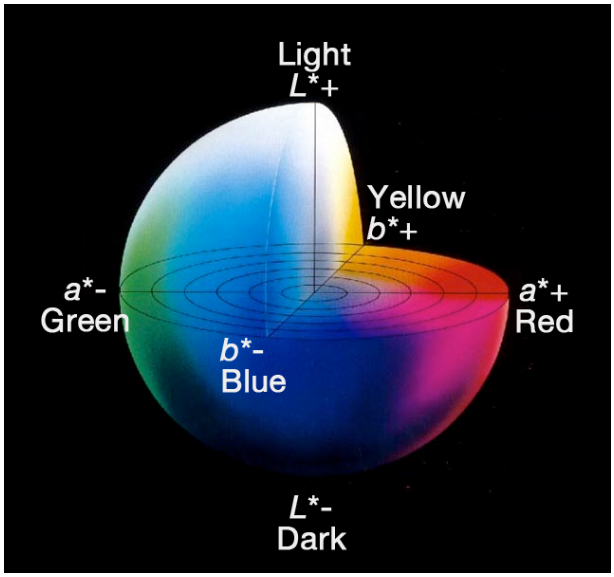

(B)

Figure 2.1 CIELab color space (A). Measurement spots were selected inside the yellow circles directly under the ischial callosities (B).

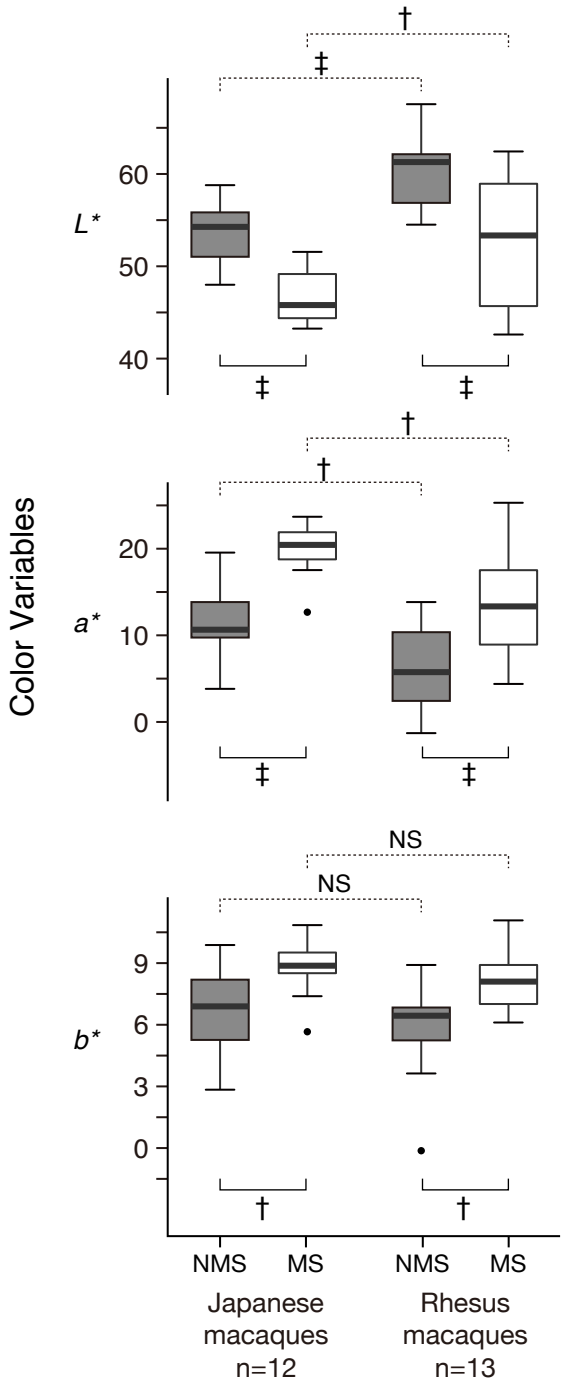

Figure 2.2 Species and seasonal differences in hindquarter coloration.

The dashed lines represent the inter-specific comparisons for each season. The black bold lines indicate the means and the black circles indicate the deviated values.

† $p < 0.01$; ‡ $p < 0.001$. NS denotes not significant.

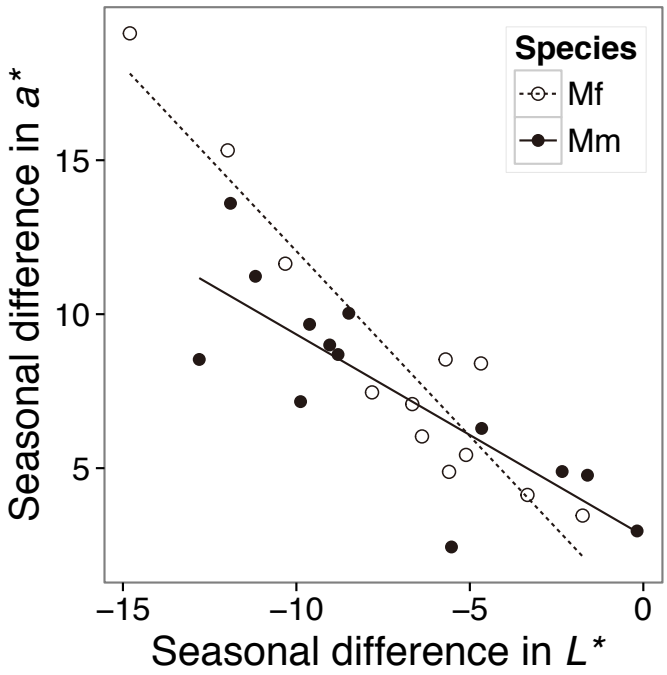

Figure 2.3 Correlation between the seasonal differences (MS - NMS) in L^* and a^* for Japanese macaques (Mf) and rhesus macaques (Mm).

Chapter 3 Relationship between skin pigments and skin color

3.1 Introduction

In Chapter 2, spectrocolorimetry results with CIELAB color space implied that melanin content can contributed to the species differences in L^* variable, and that vascularization and/or vasodilation affected seasonal change in a^* variable. Epidermal melanin content changes the L^* variable in human skin [Alaluf et al., 2002b]. However, Montagna reported that rhesus macaques had low melanin levels in epidermis [Montagna, 1966]. In Japanese macaques, although the bluish skin includes abundant melanocytes in the dermis rather than epidermis, the pinkish areas lacked melanin granules [Kimura, 2007]. These previous studies did not perform comparative quantitative examinations between seasons or between species assessing relationships between skin darkness and melanin granules in macaques. Therefore, it is unknown whether melanin granules can cause the seasonal increase and species difference in L^* variable in the macaques.

While melanin content has also been associated with skin redness [Alaluf et al., 2002b], hemoglobin content near skin surface mainly affects skin redness in human [Zonios, et al., 2001]. The seasonal increase of a^* values in figure 2.2 may be due to an increase in hemoglobin content. When hemoglobin content is increased, there are two possible consequences; vascularization/angiogenesis resulting in an increase of the number of blood capillaries and vasodilation resulting in enlargement of blood

capillaries. Both vascular factors can change hemoglobin content in sub-epidermal area and modify the a^* value. The physiological basis between the vascularization and vasodilation is different. Some growth factors, such as acidic fibroblast growth factor (FGF-1), vascular endothelial growth factor (VEGF), and angiopoietins (Ang1 and Ang2), can stimulate the formation and growth of blood vessels [Stegmann, 1998; Thurston, 2003]. On the other hand, known examples of vasodilators include protein kinase G, adenosine, endothelium-derived hyperpolarizing factor, and other biochemical mediators. [Costa and Biaggioni, 1998; Kurihara et al., 2000; Luksha et al., 2009]. The cooperation between these physiological factors and steroid hormones varies. To understand the roles of sexual skin coloration in breeding behaviors, it is important to reveal which the vascular functions, namely vascularization and vasodilation, are associated with skin redness according to internal hormonal levels, which helps to understand the function of coloration in the context of obscuring fertile periods.

In this chapter, the cutaneous factors, such as melanin content, vascularization, and vasodilation, were investigated by the image analysis and were compared quantitatively in two ways. One aimed to investigate the characteristics of hindquarter skin by comparing various skin regions. To that end, the skin was sampled in NMS at a basic condition when the hormonal surge was inactive. The other method was to assess the seasonality of the cutaneous factors in the hindquarters associated with sexual skin coloration from NMS to MS.

3.2 Materials and Methods

3.2.1 Subjects

For comparison of skin color and the cutaneous factors between various skin regions, a female Japanese macaque aged 21 years (Mf1481) was recruited. Color profiles measurements and biopsies were conducted in July 2014. For the analyses of seasonal skin coloration and the cutaneous factors, 15 female Japanese macaques aged from 4–6 years and 15 female rhesus macaques aged from 3–5 years were recruited. Color profiles measurements and biopsy in hindquarters were conducted in July (non-mating season: NMS) and October (mating season: MS) 2010, or in August (NMS) and November (MS) 2011. Two of 15 Japanese macaques were studied in 2010, 10 were studied in 2011, and the other three were both studied in 2010 and 2011. Meanwhile, six of 13 rhesus macaques were studied in 2010, another seven were studied in 2011, and the other two were studied both in 2010 and 2011.

3.2.2 Color measurement and biopsy

To perform color measurements and skin biopsies, four spots were selected: the forehead (referred to as the face), median abdomen, median dorsum (referred to as the back), and 2–3 cm below the ischial callosity of each side (referred to as the hindquarter) (figure 3.1). For the seasonal study, skin color profiles and tissues were obtained from the hindquarters. Prior to these samplings, the selected spots were cleaned and shaved. Color measurements and extraction of color variables in CIELAB

were performed in the same way as performed in Chapter 2. Each spot was measured three times. After the color measurements, biopsy was performed in the same spot with a scalpel. The size of obtained tissue was approximately 10 mm × 30 mm, and the depth was to the subcutaneous fat layer. The obtained tissue was immediately immersed in 4% phosphate buffered formalin and then embedded in paraffin.

3.2.3 Staining of tissue sections

Each tissue was cut into sections. For analyses of vascular capillaries, sections were stained with hematoxylin and eosin (HE) by New Histo. Science laboratory Co., Ltd. in Tokyo, Japan. For staining of melanin granules, sections were stained with Masson-Fontana (MF) staining using the following method in the laboratory [modified from Kwon-Chung et al., 1981]. Staining solution comprised 5% silver nitrate in aqueous solution, ammonium hydroxide, and distilled water. The paraffin sections were de-waxed in xylene and rehydrated through graduated ethanol to water. The sections were incubated in the dark at room temperature overnight. A section for negative control was incubated with phosphate buffered saline (PBS). After 15–18 h, sections were incubated in the fixing solution for three minutes (CHUGAI MY FIXER and CHUGAI MY HARDENER, Chugai Photo Chemical Co., Ltd., Tokyo, Japan). After that, sections were counter-stained with Kernechtrot Stain Solution (Muto Pure Chemicals Co., Ltd., Tokyo, Japan) and dehydrated through an ethanol series, followed by exposure to xylene and mounting. To confirm the staining of melanin granules, melanin was bleached with 3% H_2O_2 in 0.05 M PBS at 55°C for 2 h, whereby staining

for MF disappeared.

3.2.4 Image Analysis

Tissue sections were observed and digitally captured with using a light microscope with Leica system (Leica CTR 6000, Leica Microsystems GmbH, Wetzlar, Germany) for each specimen. The captured regions were randomly selected from the sub-epidermal area in the sections of skin. All images were stored at 5100 × 3800-pixeled digital files, giving a pixel resolution of about 0.46 μm. A set of NMS and MS were captured with the same settings; exposure time, gain, and white balance. Captured images were treated with Adobe Photoshop CS5 (Adobe Systems, San Jose, CA, USA). Because macaques have a uniform color vision system similar to that of humans [Jacobs and Deegan, 1999; Changizi et al., 2006], visible light wavelength is similar in catarrhines including humans, which is about 400–750 nm. Theoretically, in fair Caucasian skin, the incident light with a wavelength of 400 and 700 nm can penetrate to depths of approximately 90 and 750 μm in the skin surface, respectively [Anderson and Parrish, 1981]. As theoretical analysis has not been conducted for macaque skin, the results from human skin were adopted. The depth of the observed area was determined to be approximately 800 μm from the skin surface. The width of the observed area spanned at least 3.5 mm, which was enough to cancel the uneven localization of cutaneous factors. In the observed area, the following three cutaneous parameters were manually measured three times for each specimen: the number and lumen size of all vascular capillaries in the observed area, and the size of the

MF-stained region that reflects the melanin content. The following three indices were then calculated. First, the density of vascular capillaries in the observed area as the index of angiogenesis (was referred to as the "capillary density"). Second, the mean logarithmic lumen area size of all vascular capillaries in the observed area was the index of vasodilation/vasoconstriction (referred to as the "capillary size"). Third, the proportion of stained region with MF stain compared to the size of observed area was the index of the amount of melanin granules (referred to as the "melanin density"). The summary of image analysis is illustrated in figure 3.3.

3.2.5 Data analysis

For comparative analysis of four skin regions, the relationship between the color variables and the three cutaneous indices was plotted. The average of sexual skin coloration and the cutaneous factors between NMS and MS were tested using the paired t-test. The differences in cutaneous factors between the two species in each season were tested with the two-sample t-test and Welch's two-sample t-test, if necessary. One-sample t-test was performed to test whether the mean distribution of seasonal differences in capillary indices was significantly different or not. Regression analyses were conducted among color variables and cutaneous factors. In addition, Pearson's correlation coefficients were calculated the color variables and the cutaneous factors. A p value less than 0.05 was considered significant.

3.3 Results

For the comparison of four skin regions in basic condition, the average ± standard deviation (SD) of L^* and a^* was 43.9 ± 0.17 and 18.2 ± 0.23 in the hindquarter, 60.7 ± 0.78 and 10.3 ± 0.60 in the face, 68.4 ± 0.37 and 1.02 ± 0.04 in the back, and 62.78 ± 0.09 and −4.36 ± 0.03 in the abdomen, respectively. There were significant differences in both L^* and a^* between hindquarter and face using the two-sample t-test (L^*: t = −36.7, df = 2.19, $p < 0.001$; a^*: t = 17.7, df = 2.40, $p < 0.01$). Observed with the microscope, the sub-epidermal vascular capillaries in the hindquarter of Mf1481 appeared to be more dilated and abundant than the other three skin regions (figure 3.2). The capillary density was 7.60×10^{-5} counts/μm^2 in the hindquarter, 2.60×10^{-5} counts/μm^2 in the face, 1.00×10^{-5} counts/μm^2 in the back, and 1.38×10^{-5} counts/μm^2 in the abdomen (figure 3.4). The capillary size was 5.23 ± 1.20 μm^2 in the hindquarter, 4.44 ± 1.62 μm^2 in the face, 4.01 ± 1.01 μm^2 in the back, and 4.03 ± 1.24 μm^2 in the abdomen. The capillary size in the hindquarter was significantly greater than that in the face (t = 3.03, df = 63.46, $p < 0.01$), the back (t = 4.58, df = 22.40, $p < 0.001$), and the abdomen (t = 4.38, df = 31.60, $p < 0.001$) (figure 3.4). The melanin density ± SD was 2.74 ± 0.42 ($\times 10^{-4}$) pixels/μm^2 in the hindquarter and 222.68 ± 2.06 ($\times 10^{-4}$) pixels/μm^2 in the abdomen, whereas melanin granules were not found in the sub-epidermal region of the face and the back. As for the correlation between color variables and cutaneous factors, the capillary density was significantly correlated with L^* (r = −0.99, t = −8.31, df = 2, $p < 0.05$), but not with a^* and b^* (a^*: r = 0.89, t = 2.72, df = 2, p = 0.11; b^*: r =

0.44, t = 0.70, df = 2, p = 0.56). The capillary size was significantly correlated with L^* (r = −0.98, t = −6.66, df = 2, $p < 0.05$), but not with a^* and b^* (a^*: r = 0.90, t = 2.88, df = 2, p = 0.10; b^*: r = 0.47, t = 0.75, df = 2, p = 0.53). The melanin density was significantly correlated with b^* (r = -0.95, t = −4.34, df = 2, $p < 0.05$), but not with L^* and a^* (L^*: r = 0.23, t = 0.34, df = 2, p-value = 0.77; a^*: r = −0.70, t = −1.40, df = 2, p = 0.30).

For the seasonal analyses of cutaneous factors in the hindquarter using 15 Japanese macaques and 15 rhesus macaques, approximately 12,000 vascular capillaries in total were measured three times and analyzed. As for seasonal changes in each species, the capillary density ± SD was 6.49 ± 1.51 ($\times 10^{-5}$) counts/μm^2 in NMS and 7.86 ± 2.05 ($\times 10^{-5}$) counts/μm^2 in MS in the 15 Japanese macaques. This compared with 6.34 ± 1.55 ($\times 10^{-5}$) counts/μm^2 in NMS and 5.59 ± 1.95 ($\times 10^{-5}$) counts/μm^2 in MS in the 15 rhesus macaques. The capillary density increased only in the 15 Japanese macaques from NMS to MS (t = −2.48, df = 14, $p < 0.05$ by paired t-test; table 3.1). In addition, the capillary size ± SD was 4.25 ± 0.21 μm^2 in NMS and 4.52 ± 0.23 μm^2 in MS in the 15 Japanese macaques, whereas it was 4.13 ± 0.43 μm^2 in NMS and 4.83 ± 0.34 μm^2 in MS, in the 15 rhesus macaques. The capillary size increased from NMS to MS in both Japanese and rhesus macaques (the 15 Japanese macaques: t = −2.89, df = 14, $p < 0.05$ by paired t-test; the 15 rhesus macaques: t = −5.02, df = 14, $p < 0.001$ by paired t-test; table 3.1). The melanin density ± SD was 5.42 ± 4.45 ($\times 10^{-4}$) pixels/μm^2 in NMS and 4.37 ± 4.61 ($\times 10^{-4}$) pixels/μm^2 in MS in the 15 Japanese macaques, whereas 1.04 ± 1.03 ($\times 10^{-4}$) pixels/μm^2 in NMS and 0.41 ± 0.42 ($\times 10^{-4}$) pixels/μm^2 in

MS in the 15 rhesus macaques. The melanin density was increased only in the 15 rhesus macaques ($t = 2.34$, $df = 14$, $p < 0.05$ by t-test; table 3.1). As for species difference between the 15 Japanese macaques and 15 rhesus macaques in each season, the vascular factors were significantly different in MS (the density: $t = 3.10$, $df = 27.93$, $p < 0.01$ by two-sample t-test; the size: $t = -3.00$, $df = 24.71$, $p < 0.01$; table 3.1). Species difference in melanin density was found in NMS and MS (NMS: $t = 3.71$, $df = 15.5$, $p < 0.01$; MS: $t = 3.31$, $df = 14.24$, $p < 0.01$; table 3.1).

As for the correlation analysis between the color variables and cutaneous factors in each species, the color variables were significantly correlated with the capillary density in the 15 Japanese macaques (L^*: $r = -0.41$, $t = -2.38$, $df = 28$, $p < 0.05$; a^*: $r = 0.40$, $t = 2.34$, $df = 28$, $p < 0.05$; b^*: $r = 0.40$, $t = 2.31$, $df = 28$, $p < 0.05$). In addition, color variables correlated with the capillary size in the 15 Japanese macaques (L^*: $r = -0.42$, $t = -2.41$, $df = 28$, $p < 0.05$; a^*: $r = 0.37$, $t = 2.13$, $df = 28$, $p < 0.05$; table 3.2) and in the 15 rhesus macaques (L^*: $r = -0.57$, $t = -3.65$, $df = 28$, $p < 0.01$; a^*: $r = 0.57$, $t = 3.62$, $df = 28$, $p < 0.01$; b^*: $r = 0.54$, $t = 3.37$, $df = 28$, $p < 0.01$; table 3.2). The color variables also correlated significantly with the melanin density in the 15 rhesus macaques (L^*: $r = 0.38$, $t = 2.15$, $df = 28$, $p < 0.05$; a^*: $r = -0.46$, $t = -2.71$, $df = 28$, $p < 0.05$; b^*: $r = -0.62$, $t = -4.17$, $df = 28$, $p < 0.001$). As for species comparison of relationships between color variables and capillary size, the regression lines of the two macaque species were parallel in L^* and a^* by analyses of variance (L^*: $F = 0.031$, $p = 0.86$; a^*: $F = 0.061$, $p = 0.81$; figure 3.7). The intercepts of regression lines between color variables and capillary size in the rhesus macaques were higher than

that in the Japanese macaques (L^*: t = 5.16, df = 57, $p < 0.001$; a^*: t = −3.71, df = 57, $p < 0.001$; figure 3.7). The results of the one-sample t-test on the horizontal axis indicated the degree of vascular factors were significant for the capillary density only in the Japanese macaques (Mf: t = 2.48, df = 14, $p < 0.05$; Mm: t = −1.55, df = 14, p = 0.14) but were significant in the capillary size in both species (Mf: t = 2.89, df = 14, $p < 0.05$; Mm: t = 5.02, df = 14, $p < 0.001$) (figure 3.8).

3.4 Discussion

As shown in the comparison of four skin regions, the hindquarter of Mf1481 was the reddest and darkest even during NMS (figure 3.4). It has been previously reported that the face, that was vertex, was redder and darker than the hindquarter in Japanese macaques reared at PRI [Hamada et al., 1992]. There might be individual differences in the redness and darkness of the face and hindquarter in Japanese macaques. In this study, although not all of the correlation coefficients were significant due to low sampling sizes, the a^* and L^* tended to reflect the degree of capillary density and size among four skin regions in NMS, but was not associated with the melanin density (figure 3.4). It is of interest that the sexual skin exhibited high levels of the redness as well as the capillary density and size without a cyclical surge of sex hormones. Either or both of vascularization and vasodilation might maintain skin redness without being influenced by short-term fluctuation of sex hormone levels.

The index of vascularization, namely the capillary density, increased from NMS to MS (figure 3.5), and correlated with the a^* variable in Japanese macaques (figure 3.7 and table 3.2). Vascularization had some effects on the reddened sexual skin only in the Japanese macaques (figure 3.8). As vascularization contributes to an increase in hemoglobin content, it might explain the higher a^* variable in Japanese macaques shown in figure 2.2. It is possible that vascularization also proceeded in the rhesus macaques but the contribution to redness was obscured by other factor(s), e.g., sexual swelling. As mentioned in Chapter 4, sexual skin swelled more obviously in rhesus macaques than in Japanese macaques at PRI in this study. Sexual swelling brings about an increase in volume of sexual skin and a spatial dispersion of vascular capillaries structurally. Even if vascularization proceeds in rhesus macaques, the spatial dispersion by sexual swelling might counteract the increasing capillary density by vascularization, which does not affect redness. Vascularization may contribute to the redness of sexual skin only in the Japanese macaques whose sexual skin swells less obviously than rhesus macaques.

The capillary size, which is the index of vasodilation/vasoconstriction, increased from NMS to MS (figure 3.5B and table 3.1) and correlated with the L^* and a^* variables in both the Japanese macaques and the rhesus macaques (figure 3.7 and table 3.2). As for species comparison between NMS and MS, the t value of the rhesus macaques was higher than that of the Japanese macaques, and the capillary size were higher in the rhesus macaques than in the Japanese macaques in MS (figure 3.5). Therefore, the effects of vasodilation may be greater in rhesus macaques than in

Japanese macaques. Although there was species difference in the degree of vasodilation, the vasodilation was common phenomenon in both species (figure 3.8). Vasodilation/ vasoconstriction may mainly modify seasonal coloration of sexual skin in Japanese macaques and rhesus macaques.

Melanin density was much larger in the Japanese macaques than the rhesus macaques (figure 3.5C and 3.6). The species difference in melanin content between the two macaques may explain the species difference in L^* in figure 2.2 in Chapter 2. Abundant melanin in the Japanese macaques may support the observation of them having darker hindquarters. However, melanin density was not associated with the seasonal change of L^* in the Japanese macaques (figure 3.7 and table 3.2). In contrast, the correlation coefficients between the melanin density and L^* was significant but positive in the rhesus macaques (figure 3.7 and table 3.2). If melanin content is increased in skin, skin color becomes dark; therefore, L^* is decreased and the correlation coefficient between the melanin content and L^* shows a negative value [Takiwaki, 1998; Alaluf et al., 2002a]. Therefore, the positive correlation coefficients in the rhesus macaques do not explain the seasonal decrease in L^*. Because the seasonal differences of L^* and a^* were significantly correlated (figure 2.3), the same factor(s) may modify the both seasonal coloration. The L^* was significantly correlated with the capillary density and size in the Japanese macaques and with the capillary size in the rhesus macaques (figure 3.7 and table 3.2). The vascular factors might increase the darkness in MS. Melanin content may support species difference in sexual skin darkness through NMS and MS; nevertheless, it did not modify seasonal sexual skin

coloration in the macaques.

It is noticeable that both vascularization and abundant melanin were observed only in Japanese macaques, whereas vasodilation was observed in both species. The physiological processes involved in vasodilation are short-term, for instance, nitric oxide is known as a powerful vasodilator with a short half-life of a few seconds [Moncada et al., 1991] and can be mediated with 17β-estradiol through nongenomic pathway [Chen et al., 1999]. In contrast, the processes involved in vascularization and melanin production are comparatively long-term. The long-term factors may promote an escalation of redness and darkness in the Japanese macaques through MS. The short-term and long-term factors acted in combination in affecting sexual skin coloration in the Japanese macaques. In contrast, sexual skin coloration in the rhesus macaques was due to a single short-term factor in regard to pigments—vasodilation. However, it would be premature to conclude that only vasodilation/vasoconstriction generates an honest cue for fertile periods according to hormonal conditions. The structural changes induced by sexual swelling may also modify skin color. The effect of swelling on coloration is discussed in Chapter 4. As for skin pigments in Japanese macaques, vasodilation as the short-term factor and vascularization and abundant melanin as the long-term factors worked together in sexual skin coloration, which may produce a broad signal for a fertile period.

In conclusion, vasodilation can commonly modify sexual skin redness in both Japanese and rhesus macaques. The vascularization in Japanese macaques may support observed species differences in redness through the year. Melanin granules did not alter

seasonal skin coloration but supported species difference with respect to darkness. The Japanese macaques were affected by a combination of long- and short-term factors, whereas the rhesus macaques were affected by a short-term factor in relation to skin pigments examined in this study. In addition to skin pigments, a structural change by sexual swelling may modify sexual skin coloration in rhesus macaques. The histological investigations of coloration will provide evolutionary insights into sexual skin development in primates.

Table 3.1

Seasonal and species differences of three cutaneous factors

	IN	SAMPLE SIZE	CAPILLARY DENSITY (counts/μm^2)	CAPILLARY SIZE (Log, μm^2)	MELANIN DENSITY (pixels/μm^2)
Seasonal difference	Mf	15	**2.48**$^{\#}$ (**2.22**$^{\#}$, 1.86)	**2.89**$^{\#}$ (**2.36**$^{\#}$, **2.24**$^{\#}$)	1.16 (0.85, 1.76)
	Mm	15	1.55 (1.18, **2.5**$^{\#}$)	**5.02**‡ (**4.96**‡, **4.41**‡)	**2.34**$^{\#}$ (**2.34**$^{\#}$, **2.36**$^{\#}$)
Species difference	NMS	15	0.27 (0.61, 0.53)	0.96 (1.61, 0.66)	**3.71**† (**3.02**$^{\#}$, **2.76***)
	MS	15	**3.10**† (**2.88**†, **3.16**†)	**3.00**† (**2.65**$^{\#}$, **2.84**†)	**3.31**† (**2.85**$^{\#}$, **2.65***)

Upper two rows: inter-season comparisons of capillary density, capillary size and melanin density in each species. Lower two rows: inter-species comparisons of the same factors in each season. Figures represent absolute t values by paired t-test or Welch's two-sample t-test. Bold numbers indicate significant values. The figure that is not included in parentheses is the result of all specimens, whereas the two figures in the parentheses are the t values of samples without duplicated specimens in 2011 (the former) or 2010 (the later).
# $p < 0.05$; † $p < 0.01$; ‡ $p < 0.001$. Mf: Japanese macaques; Mm: Rhesus macaques; NMS: non-mating season; MS: mating season.

Table 3.2

Correlations between color variables and three cutaneous factors in each species

SPECIES	CIELAB	SAMPLE SIZE	CAPILLARY DENSITY	CAPILLARY SIZE	MELANIN DENSITY
Mf	*L**	30	**−0.41**$^{\#}$ (−0.33, −0.38)	**−0.42**$^{\#}$ (−0.3, **−0.54**†)	0.12 (0.22, −0.041)
	*a**	30	**0.40**$^{\#}$ (0.37, 0.35)	**0.37**$^{\#}$ (0.23, **0.49**$^{\#}$)	**−0.37**$^{\#}$ (−0.40, −0.28)
	*b**	30	**0.40**$^{\#}$ (0.40, **0.42**$^{\#}$)	0.28 (0.19, 0.39)	−0.26 (−0.21, −0.17)
Mm	*L**	30	−0.20 (−0.18, −0.23)	**−0.57**† (**−0.61**†, **−0.53**†)	**0.38**$^{\#}$ (0.34, **0.39**$^{\#}$)
	*a**	30	0.24 (0.21, 0.24)	**0.57**† (**0.62**‡, **0.51**†)	**−0.46**$^{\#}$ (**−0.42**$^{\#}$, **−0.47**$^{\#}$)
	*b**	30	0.01 (−0.04, −0.12)	**0.54**† (**0.56**†, **0.49**†)	**−0.62**‡ (**−0.63**‡, **−0.70**‡)

Figures indicate Pearson's correlation coefficients. Bold figures indicate significant values. The figure that is not included in parentheses is the result of all specimens, whereas the two figures in the parentheses are the t values of samples without duplicated specimens in 2011 (the former) or 2010 (the later). # $p < 0.05$; † $p < 0.01$; ‡ $p < 0.001$. Mf: Japanese macaques; Mm: Rhesus macaques.

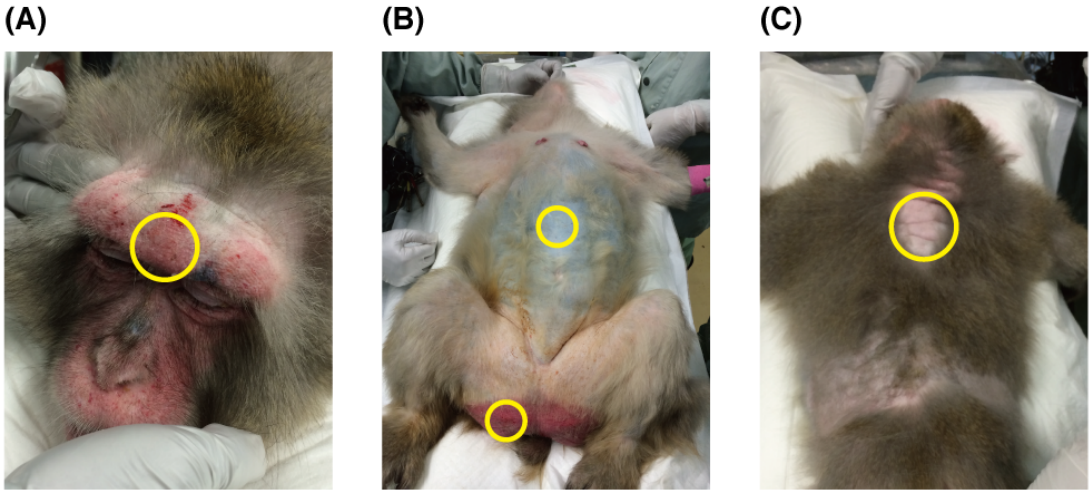

Figure 3.1 Selected measurement spots indicated by yellow circles on the face (A), hindquarter and abdomen (B), and the back (C) of a Japanese macaque (Mf1481).

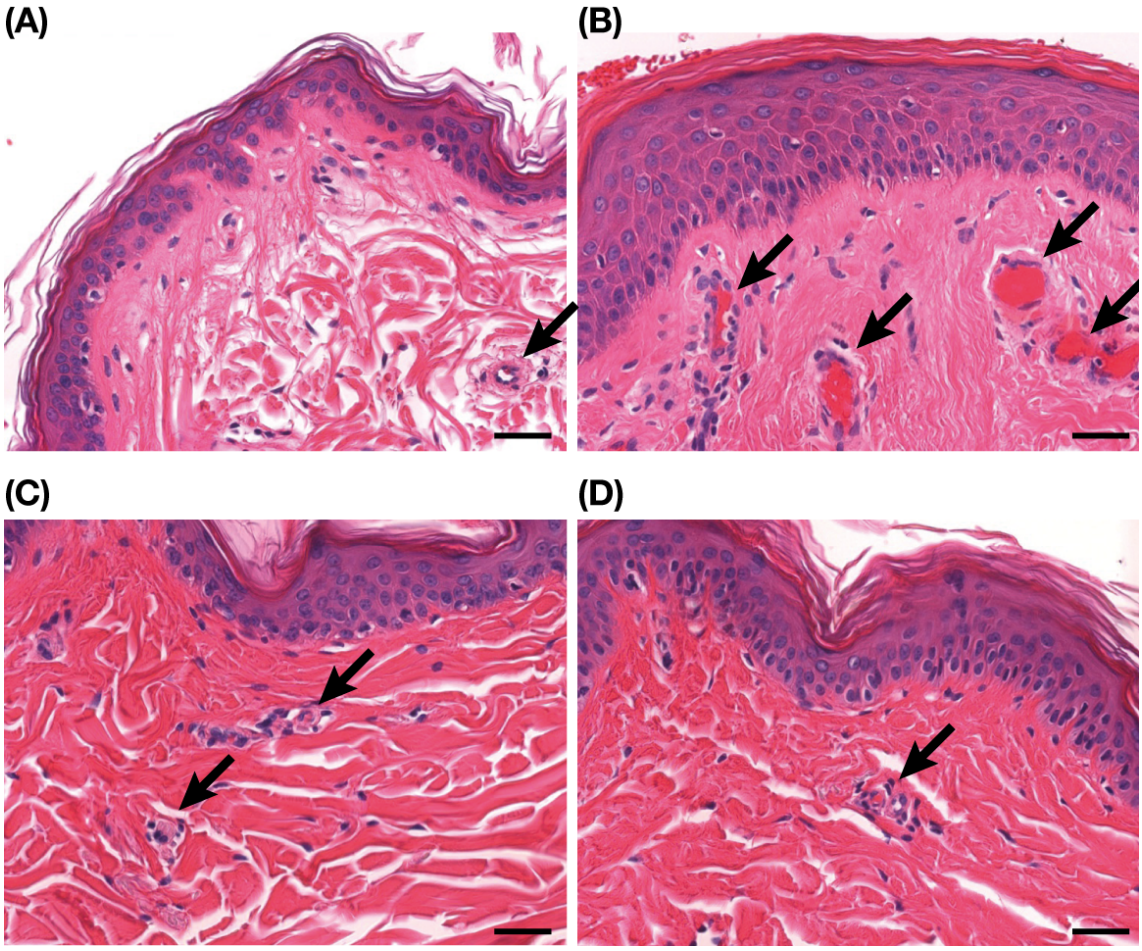

Figure 3.2 Sections of four skin regions of Mf1481; face (A), hindquarter (B), abdomen (C), and back (D). Arrows represent vascular capillaries. Bars, 25 µm; hematoxylin and eosin stain.

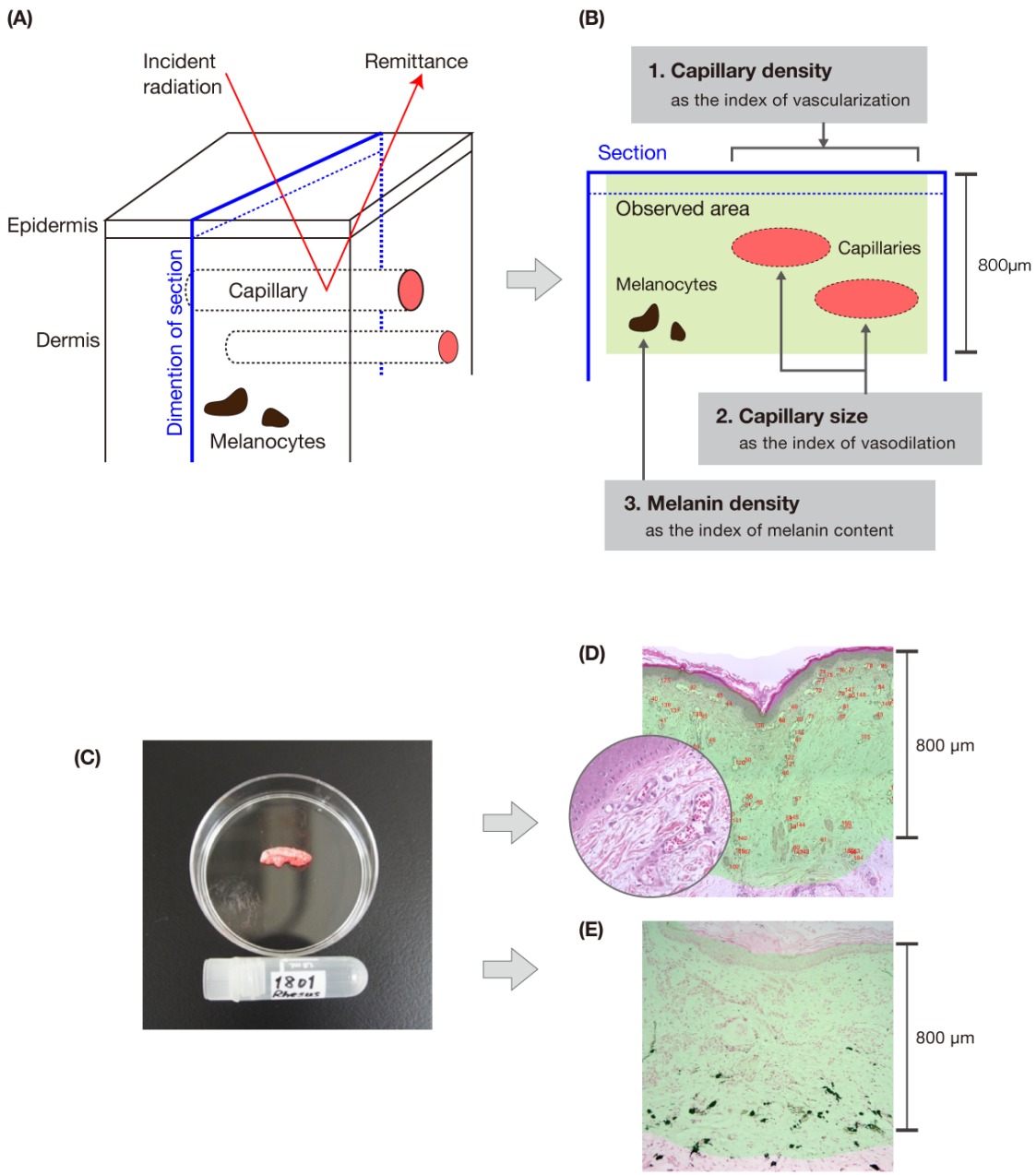

Figure 3.3 Illustration of image analysis (A, B), biopsied skin (C), HE stained section (D) and MF stained section (E). Observed area (800 μm from skin surface) is represented in green (B), (D) and (E). Enlarged image is shown in inset area in (D). Vascular capillaries are numbered with small, red colorations in (D).

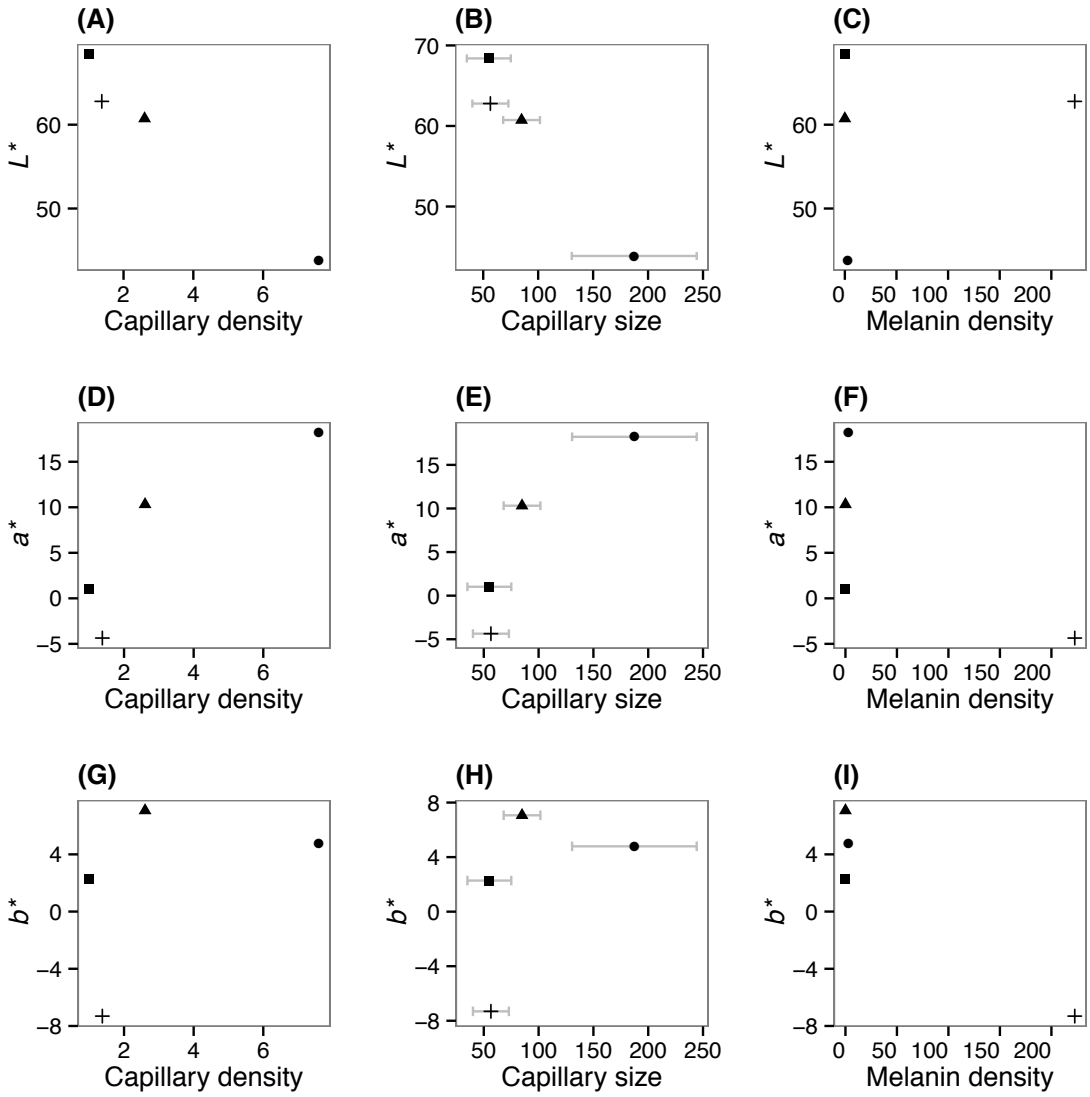

Figure 3.4 Relationship between three cutaneous factors (capillary density (× 10^{-5} counts/μm^2), capillary size (μm^2), and melanin density (× 10^{-4} pixels/μm^2)) and three color variables (*L**, *a**, and *b**). Error bars indicate standard deviations, whereas standard deviations of measurements for color data were so small and not shown in the figures. ●: hindquarter, ▲: face, +: abdomen, ■: back.

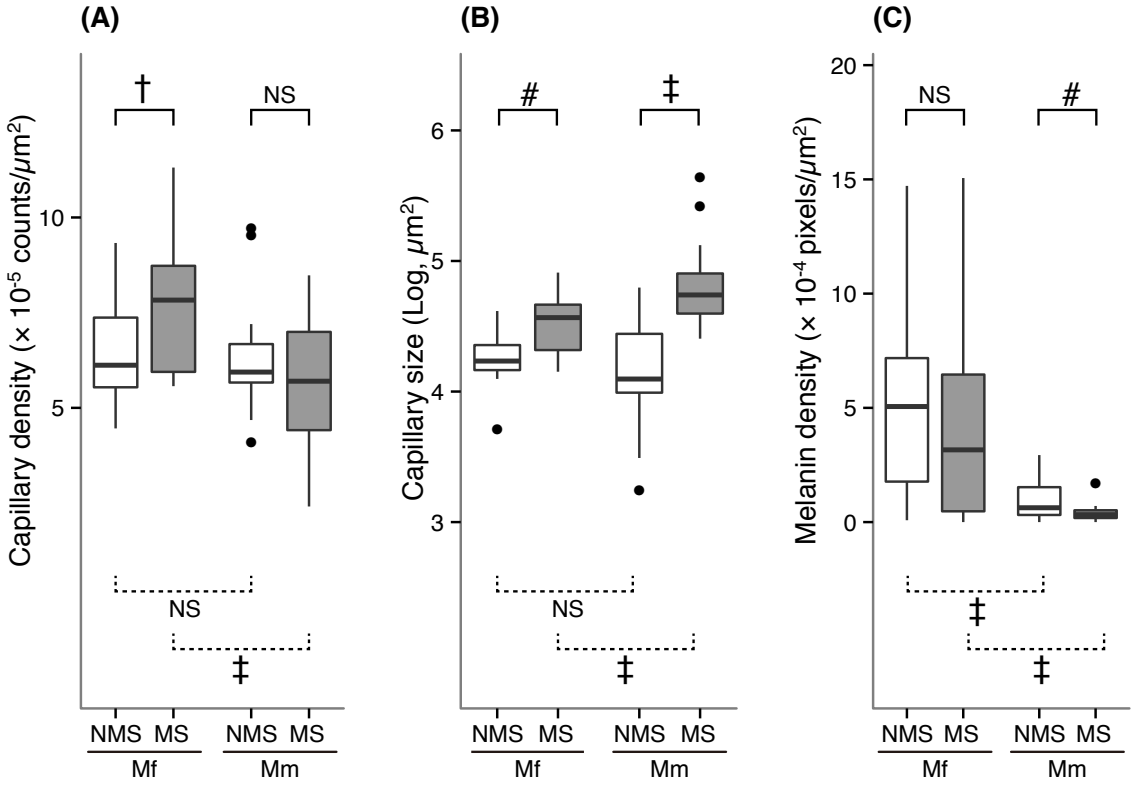

Figure 3.5 Seasonal comparison of three cutaneous factors; capillary density, capillary size, and melanin density. The upper and lower "hinges" correspond to the first and third quartiles (25% and 75%). The lower whisker extends from the hinge to the lowest value within 1.5 * IQR of the hinge, where IQR is the first quartile subtracted from the third quartile. The upper whisker extends from the hinge to the highest value that is within 1.5 * IQR of the hinge. Data beyond the end of the whiskers are outliers and plotted as circular points. The black bold lines in the boxes indicate medians. # $p < 0.05$; † $p < 0.01$; ‡ $p < 0.001$. NS denotes not significant.

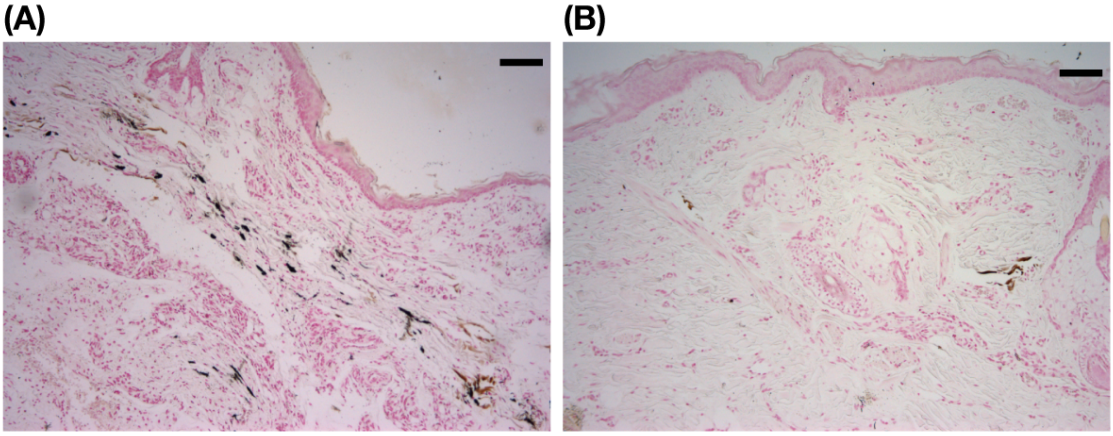

Figure 3.6 Sections of hindquarter of Mf2121 (A) and Mm1795 (B) in NMS. Black and brown stained regions represent localization of melanin granules. Bars, 100 μm; Masson–Fontana stain.

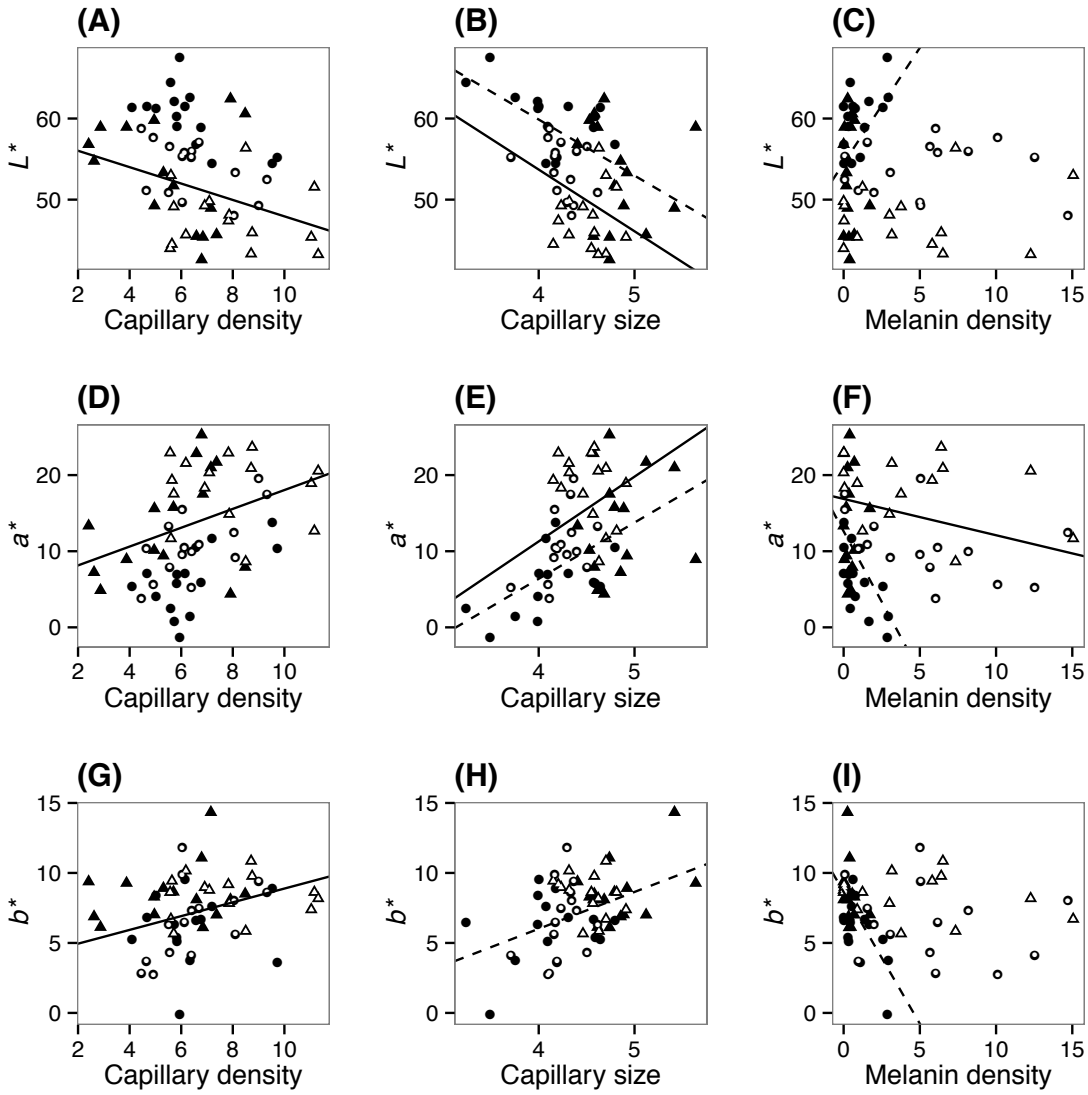

Figure 3.7 Relationship between three cutaneous factors (capillary density (× 10^{-5} counts/μm^2), capillary size (Log, μm^2), and melanin density (× 10^{-4} pixels/μm^2)) and three color variables (*L**, *a**, and *b**). Solid lines indicate significant regression lines for 15 Japanese macaques and dashed lines indicate significant regression lines for 15 rhesus macaques. ○: Mf in NMS; △: Mf in MS; ●: Mm in NMS; ▲: Mm in MS.

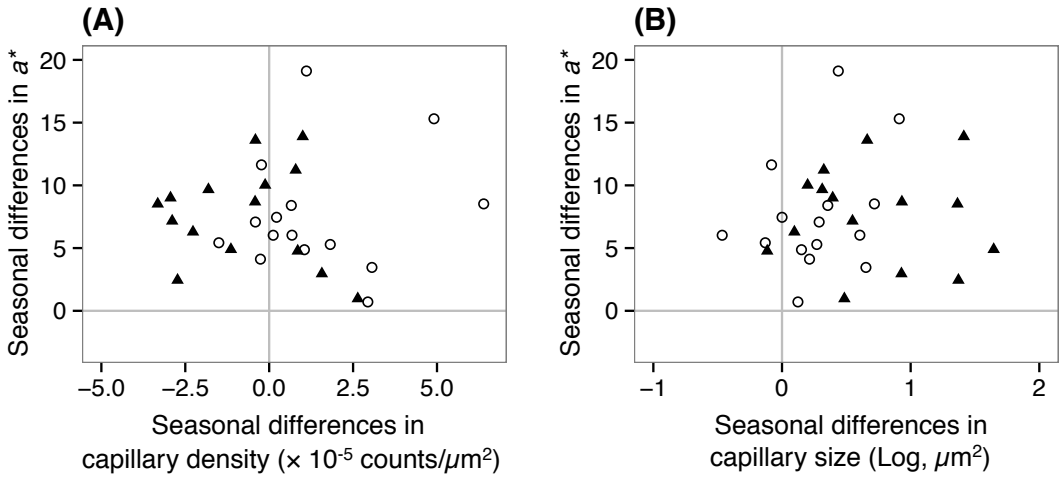

Figure 3.8 Relationship between seasonal differences in *a** and the vascular factors. Blank circles (◯) indicate Japanese macaques and filled triangles (▲) indicate rhesus macaques.

Chapter 4 Relationship between skin hyaluronan and skin color

4.1 Introduction

It has been reported that adolescent females of both Japanese and rhesus macaques exhibit sexual swellings [Anderson and Bielert, 1994]. However, in this study, none of the 15 Japanese macaques aged between 4–6 years exhibited sexual swelling, whereas 12 of the 15 rhesus macaques aged between 3–5 years did have sexual swelling. Whether sexual swelling is found in Japanese macaques depends on the extrinsic environment, such as availability of nutrition [Mori et al., 1997]. In addition, incidence of ovulatory cycles is at least partly dependent on both temperature and photoperiodicity in Japanese and rhesus macaques [Nozaki et al., 1992]. In this study, the Japanese macaques and the rhesus macaques were reared in the same conditions and on the same diet. Therefore, the species difference in sexual swelling indicates that it develops more weakly in Japanese macaques than in rhesus macaques, in the same rearing environments. The species difference in structural changes induced by swelling can affect sexual skin color.

When the degree of swelling was previously analyzed, direct measurement of the swollen region by a measuring tape, simple grading by apparent observation, or quantification by a chemical method were employed [Wildt et al., 1977; Bentley et al., 1971]. The methods using measuring tape and observations were not suitable for assessing the link between swelling and color of the sexual skin, because local skin

color reflects the sub-epidermal components at that region. The chemical quantification using homogenized samples is inadequate for histological examination of skin structure. Therefore, skin coloration should be examined in conjunction with histological changes involved in sexual swelling. When sexual skin was swollen by artificial induction of estradiol (E2), collagen fibers in the dermis became more dispersed, the amount of hyaluronan (hyaluronic acid; HA) increased, the stratum corneum became thinner, and fibroblasts became large [Bentley, et al., 1971; Carlisle et al., 1981; Bentley et al., 1986]. Among these, HA is one of the glycosaminoglycans, which is abundant in the skin. HA and fibers such as collagen form the matrix of the dermis and subcutaneous connective tissue. Increasing HA occupies a large hydrated volume and may induce cutaneous permeability of light thereby affecting skin color. However, the effect of HA on seasonal sexual skin coloration was previously unknown.

When HA was histologically examined, HA was specifically stained and microscopic images were digitally obtained and binarized. However, it is possible that subjective bias can be introduced when the observer fixes the threshold of binarization. To avoid this bias, I have employed the Homology Image Analysis.

4.2 Materials and Methods

4.2.1 Subjects

Seven Japanese macaques aged 4–6 years, and eight rhesus macaques aged 3–

4 years were recruited in this study. Color profiles and biopsy in hindquarters were conducted in July (non-mating season: NMS) and October (mating season: MS) 2010, or in August (NMS) and November (MS) 2011. Three of the seven rhesus macaques were sampled in 2010 (Mm1798, Mm1800, and Mm1804); other three were sampled in 2011 (Mm1789, Mm1843, and Mm1846); the other was sampled both in 2010 (Mm1792a) and 2011 (Mm1792b). All seven Japanese macaques (Mf2099, Mf2115, Mf2142, Mf2152, Mf2178, Mf2189, and Mf2191) were sampled in 2011. This study followed the Guidelines for the Care and Use of non-Human Primates in the Primate Research Institute, Kyoto University and was approved by the institutional ethics committee for animal experiments.

4.2.2 Color Measurement and Biopsy

To measure sexual skin coloration, a spot 2–3 cm below the ischial callosity was selected on one side (i.e., one spot per subject per season). Prior to measurement, the subjects were anesthetized using ketamine hydrochloride (Ketalar® at 2.5 mg/kg; Sankyo-Parke-Davis & Co., Inc., Tokyo, Japan) and medetomidine hydrochloride (Domitor® at 0.1 mg/kg; Meiji Seika Kaisha, Ltd., Tokyo, Japan), after which the designated measurement areas were cleaned and shaved prior to sampling. Color measurements and extraction of the color variables L^*, a^* and b^* in CIELAB color space were performed using a spectrocolorimeter as described in Chapter 2. After the color measurements, biopsies of the same selected spot were performed as described in Chapter 3. The collected tissue samples were approximately 10 mm × 30 mm in size,

and the sampling depth extended to the subcutaneous fat layer. The obtained tissues were immediately immersed in 4% formalin in phosphate-buffered saline (PBS) and subsequently embedded in paraffin.

4.2.3 Hyaluronan Staining

Each tissue was cut into sections. These sections were stained according to the colloidal iron method. Briefly, paraffin sections were de-waxed in xylene and rehydrated through a graduated ethanol series to water. Next, the sections were soaked in 12% acetic acid for 30 s, and were incubated in a working colloidal iron solution comprising 25% colloidal iron (Cat. No. 33031; Muto Pure Chemical Co., Ltd., Tokyo, Japan), 30% acetic acid, and distilled water for 60 min. After washing with 12% acetic acid, the sections were incubated for 20 min in a 1% hydrochloric acid–potassium ferrocyanide solution. The sections were counterstained with Krnechtrot stain and dehydrated through an ethanol series, followed by exposure to xylene and mounting. To test the specificity of HA staining, I treated a section from a Japanese and a rhesus macaque (Mf2178 and Mm1846 in 2011) in MS with hyaluronidase from ovine testis (Cat. No. 25118; Cosmo Bio Co., Ltd., Tokyo, Japan) [0.5 mg/ml in PBS] for 1 h at 37°C, followed by alcian blue staining at pH 2.5 (Cat. No. 20121; Muto Pure Chemical Co., Ltd., Tokyo, Japan).

4.2.4 Mathematical Tools for Homology Image Analysis

Homology-based image analysis has been recently applied to diagnostic

procedures, such as automatic tumor detection [Nakane et al., 2013; Nakane et al., 2015]. Homology is a branch of mathematics that can be used to express the degree of contact. The *Betti numbers* are important numbers that represent the idea of homology. In two-dimensional cases, the *Betti numbers* comprise two numbers. One is *b0* (*0-dimensional Betti number*), or the number of isolated solid components, and the other is *b1* (*1-dimensional Betti number*), or the number of areas surrounded by the boundary. Essentially, as the components (*b0*) fuse with each other through contact, components (*b1*) with surrounding areas are created. Please see figure 4.2 for an example. Accordingly, I binarize images to calculate *Betti numbers*; in these images, the numbers of the black and white areas are *b0* and *b1*, respectively. This suggests that *b0* represents the HA localized regions. During sexual swelling, HA levels increase, leading to an infiltration of dispersed fibers [Carlisle et al., 1981]. When an image of HA infiltration is binarized, the infiltrated area is not entirely replete with black regions because many white regions (*b1*) also appear. Therefore, *b0* and *b1* can be used to express the degree of region contact. Consequently, when the stained areas increase, *b0* decreases, whereas *b1* inversely increases. This implies a significant increase in the *b1*/*b0* ratio.

4.2.5 Pre-analysis for Homology Image Analysis

Captured regions were randomly selected from the sub-epidermal area in the sections of skin. An image was captured using a light microscope with Leica system (Leica CTR 6000) for each specimen. All images were stored at 5100 × 3800-pixeled digital files, giving a pixel resolution of about 0.46 μm. A sample set of NMS and MS

of a specimen was captured with the same settings; exposure time, gain, and white balance. An image of a rhesus macaque (Mm1792 in 2010) during MS was used for testing homology image analysis. First, color channels were separated and blue color indicating the localization of HA was visualized from the microscopic image with Adobe Photoshop CS5 Extended. Second, the extracted image was binarized at thresholds of five degrees between 145 and 255. To test the appropriate number of divisions for homology analysis, the binarized image was divided into 1–64 sections (1 × 1, 2 × 2, 3 × 3, 4 × 4, 6 × 6, 8 × 8, 16 × 16, 32 × 32, and 64 × 64). The *b1*/*b0* ratio was calculated for each division using CHomP software (http://chomp.rutgers.edu/Project.html). The hyaluronan index (HA index) was defined as the number of sections where the ratio *b1/b0* was higher than the criteria. I tested the criteria between 0.01–2.0.

4.2.6 Homology Image Analysis and Data Analysis

Three microscopic images were obtained for each specimen and binarized at various thresholds, depending on the staining conditions. The NMS and MS image sets for each subject were obtained using the same microscope settings (exposure time, gain and white balance) and binarized at the same threshold. Binarized images were separated into 4 × 4 divisions. Finally, I counted the number of divisions wherein the *b1*/*b0* ratio exceeded 0.5 as the HA index. The average ± standard deviation (SD) of the HA index was calculated for each specimen. Changes in the HA index between the NMS and MS in each species were assessed using the paired t-test. Correlations

between the color variables (L^*, a^* and b^*) and HA indices were analyzed using linear regression. A p value < 0.05 was considered statistically significant.

4.3 Results

For the test staining of HA, hyaluronidase pre-treatment eliminated alcian blue staining. In the pre-analyses, the number of pixels in which the values exceeded thresholds easily fluctuated when the threshold was gradually changed without homology image analysis (figure 4.3A). By contrast, as with homology image analysis, HA indices at specific condition with the division at 3 × 3 and 4 × 4 sections and the criteria between 0.4–0.6 were robust for thresholds between 200 and 215 (figure 4.3B, C).

Sexual swellings were apparently not observed in any of the seven Japanese macaques, but were observed in six of the eight rhesus macaques (the observed swelling status is represented by +/–signs in figure 4.4A). Individual HA index was increased in a Japanese macaque (Mf2191: $t = 4.02$, $df = 2.94$, $p < 0.05$ by Welch's two-sample t-test) and in six of the eight rhesus macaques (Mm1792a: $t = 6.86$, $df = 2.16$, $p < 0.05$; Mm1792b: $t = 11.31$, $df = 4$, $p < 0.001$; Mm1798: $t = 32.53$, $df = 4$, $p < 0.001$; Mm1800; $t = 9.41$, $df = 2$, $p < 0.05$; Mm1804: $t = 12.12$, $df = 2$, $p < 0.01$; Mm1846: $t = 4.24$, $df = 4$, $p < 0.05$ by Welch's two-sample t-test). HA indices of the rhesus macaques and the Japanese macaques in NMS and MS are visualized in figure 4.4A. HA indices

were higher in the rhesus macaques than in the Japanese macaques (figure 4.4B). In Japanese macaques, the average ± SD of HA indices was 0.33 ± 0.56 in NMS and 1.67 ± 1.40 in MS, respectively, whereas in the rhesus macaques, the average ± SD of HA index was 0.22 ± 0.27 in NMS, and 10.33 ± 5.87 in MS, respectively (figure 4.4B). Only in the rhesus macaques was a significant seasonal difference observed ($t = -3.65$, $df = 15$, $p < 0.01$ by paired t-test).

Correlations between HA index and color variables were represented in figure 4.5. In the Japanese macaques, no significant correlation was found either in NMS or MS. In the rhesus macaques, the correlation coefficients were significant for L^* and a^* during not NMS but MS (L^*: $r = 0.91$, $r^2 = 0.83$, $t = 4.93$, $df = 6$, $p < 0.01$; a^*: $r = -0.85$, $r^2 = 0.73$, $t = -2.99$, $df = 6$, $p < 0.05$; b^*: $r = -0.042$, $r^2 = 0.002$, $t = -0.11$, $df = 6$, $p = 0.93$), when an outlier (Mm1789) was excluded. Mm1789 did not exhibit sexual swelling and HA indices in NMS and MS were low.

4.4 Discussion

The pre-analysis confirmed data rigor for thresholds with 3 × 3 and 4 × 4 divisions and criteria between 0.4–0.6 (figure 4.3B, C). The plots of HA indices flattened at a set threshold between 200 and 215 in the settings. Because the HA indices were robust with these settings, homology image analysis eliminated any subjective error involved in determining the binarization thresholds (figure 4.3). This study was

the first to adopt homology image analysis for measuring amounts of HA in skin, which avoids subjective bias. The settings were applied to the following analyses.

I observed a remarkable seasonal increase in the mean HA indices in six of eight rhesus macaques. The induction of HA biosynthesis was previously shown in the sexual skin of estrogen-treated rhesus macaques [Bentley, et al., 1971]. Thus, a seasonal increase of estrogen in MS may promote HA biosynthesis in this study. In contrast, HA indices increased during MS in one of seven Japanese macaques (figure 4.4). As a previous study reported that sexual swelling was also found in adolescent female Japanese macaques [Anderson and Bielert, 1994], it would appear that Japanese macaques also have a mechanism of sexual swelling. The two macaque species would be expected to share the basic mechanisms of sexual swelling. However, the species difference in the HA content during MS suggests that the degree of HA synthesis varies between the species, despite the same rearing conditions.

In some specimens, such as Mm1800 and Mm1843, the HA indices were inconsistent with apparent swelling. The HA index of Mm1843 was low during MS, but they did show sexual swelling. As the sampling spots were approximately 2–3 cm^2, and may be considered small, it was likely that the sampled region was not very swollen. Mm1800 had a high HA index but did not exhibit sexual swelling. Swelling may not be apparent despite increases in HA if other factors do not influence swelling conditions. For example, it might be that fibers do not disperse and instead form bundles [Carlisle et al., 1981]. Even in such cases, an increase in HA results in a concomitant increase in the water content and permeability of the skin, which modifies the skin color. Colloidal

iron staining and homology image analysis revealed fluctuations in HA that could not be determined based only on appearance.

A positive significant correlations was observed between the HA index and L^* variable, and a negative significant correlations was observed between the HA index and a^* variable in the rhesus macaques only during MS (figure 4.5). In other words, seasonal increases in HA prompted sexual skin color to lose both darkness and redness. An increase in HA induces increases in the hydrated volume and cutaneous permeability of the skin; therefore, the L^* variable may be increased and the skin color may lighten. Additionally, increased HA leading to sexual swelling and spatial dispersion of skin components may decrease the density of vascular capillaries; therefore, a^* is decreased and consequently the skin color loses redness. As a result, the effect of increased HA opposes the seasonal coloration, which generally becomes darker (decreasing L^*) and redder (increasing a^*). Because the size of sexual skin changes gradually [Nunn, 1999], HA levels may also change gradually. This suggests that fluctuation of the HA level is a long-term response compared with vasodilation. Therefore, increased HA may lower redness and darkness through MS, which may obscure color fluctuation by short-term vasodilation/vasoconstriction in rhesus macaques during MS. When the results in this chapter were considered together with the results in Chapter 3, the vascularization and abundant melanin increase the darkness and redness in the Japanese macaques, whereas the increase of HA decreased the darkness and redness in the rhesus macaques. Therefore, the species differences in the L^* and a^* variables in figure 2.2 may reflect the various coloration for each species. In

addition, it is noteworthy that the different long-term factors to alter the coloration in the two macaque species may contribute to broad signals of fertility.

A previous study has reported that face color was considered as a comparatively honest signal for fertile periods compared to the hindquarter in the rhesus macaques, because the peak of color fluctuation in the face coincided with fertile period, but the color fluctuation did not show a clear peak in the hindquarter in rhesus macaques [Dubuc et al., 2009]. With regard to the obscuring effect of HA on sexual skin coloration, the face does not swell and contains a lower amount of HA than the hindquarter, face color is more likely to reflect the seasonal changes in cutaneous factors, such as vascular capillaries depending on internal hormonal levels. Although it would be better for male rhesus macaques to interpret face color as information for assessing the probability of ovulation, these animals paid more attention to reddening of hindquarters than that of face [Waitt et al., 2006]. Thus, male rhesus macaques appear to have a preference for hindquarter color.

In conclusion, the changes in HA levels in macaques were indexed and objectively analyzed using colloidal iron staining and homology image analysis, rather than by appearance alone. I found that during MS, the HA level was increased in rhesus macaques but not in Japanese macaques. This species difference may reflect the degree of HA synthesis under the same rearing environments, despite the two macaque species being reported to show similar sexual swelling. The long-term changing HA levels in rhesus macaques counter-acted the effect of seasonal reddening and darkening induced by the short-term vasodilation. The Japanese macaques might use vascularization and

abundant melanin to obscure fertile periods (Chapter 3), whereas the rhesus macaques might use an increase in HA to for the same purpose. The two macaque species may share basic mechanisms of sexual swelling but the degree of changes may be different between the species. Further examination of hormonal regulation of sexual skin will provide insights into relationships between sexual skin swelling, coloration, and breeding behavior in primates.

Figure 4.1 Rhesus macaques without sexual swelling (left; Mm1789) and with sexual swelling as evidenced by the folds of skin (right; Mm1792).

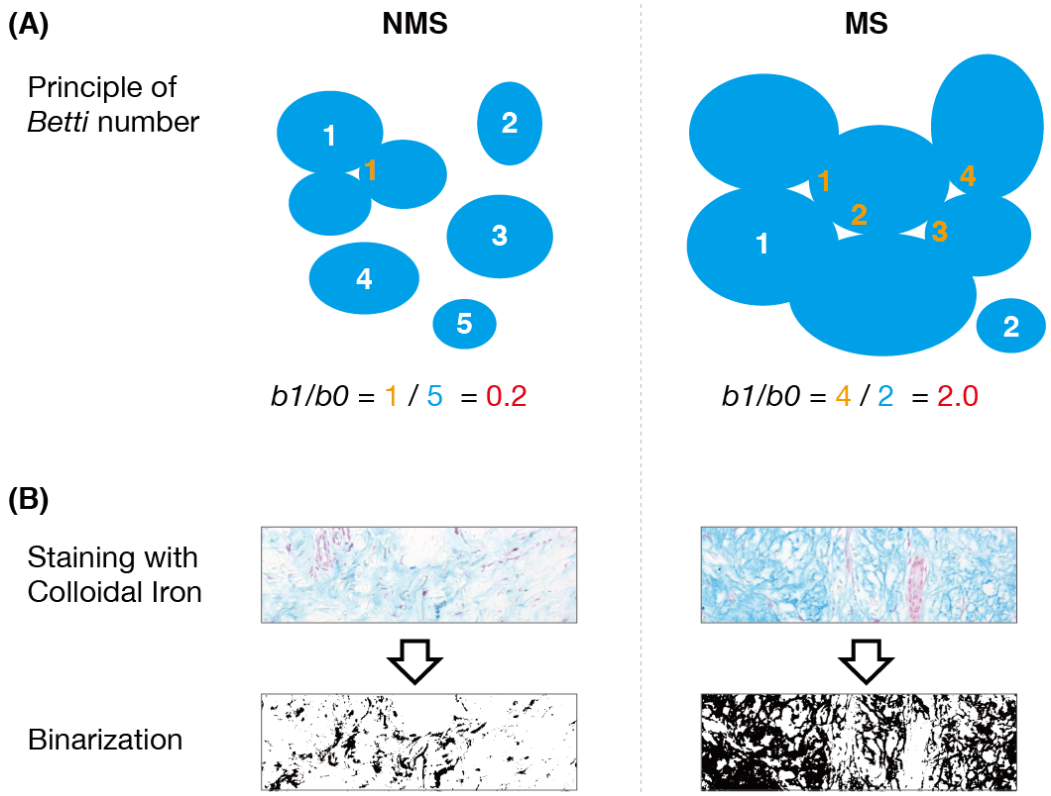

Figure 4.2 Principle of *Betti* number and homology image analysis. Blue regions indicate localization of HA. When HA levels increased from NMS to MS, the blue regions expand, which results in a decrease in the number of independent HA regions (*b0*) and an increase in the number of windows (*b1*). Consequently, the HA index (*b1*/*b0*) is increased from NMS to MS (A). A captured image of the slides is stained with colloidal iron and binarized at an appropriate threshold. Counter staining was conducted with Kernechtrot Stain Solution. The number of black regions and the number of white windows in binarized images are automatically counted to calculate the HA index using CHomP software.

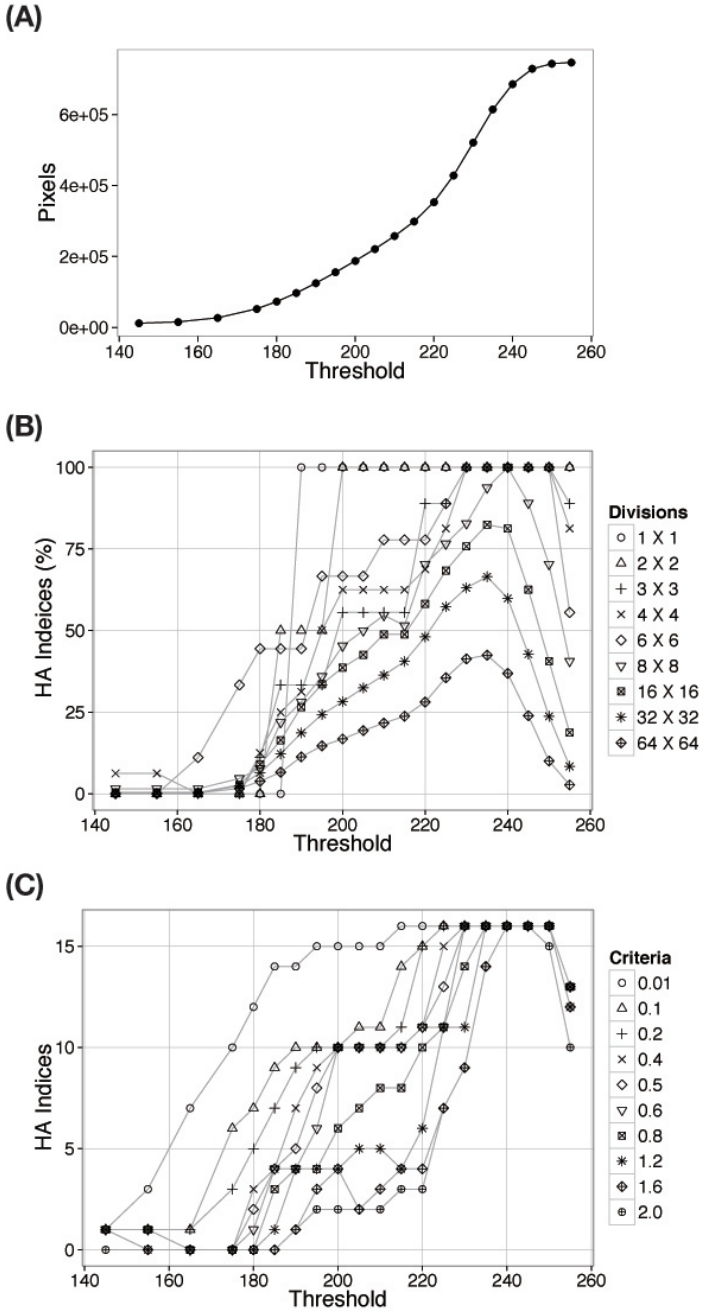

Figure 4.3 Pre-experiments using sample sections from a rhesus macaque without homology image analysis (A) and with homology image analysis (B, C). The number of pixels in a binarized image is displayed when the threshold was gradually changed in the absence of homology image analysis (A). Pre-analysis to fix the number of divisions in the homology image analysis was conducted (B). Pre-analysis to fix the criterion for *b1/b0* was conducted (C). Plots of hyaluronan indices, which indicate the degree of swelling, were flattened at a threshold between 200 and 215 and at criteria between 0.4 and 0.6.

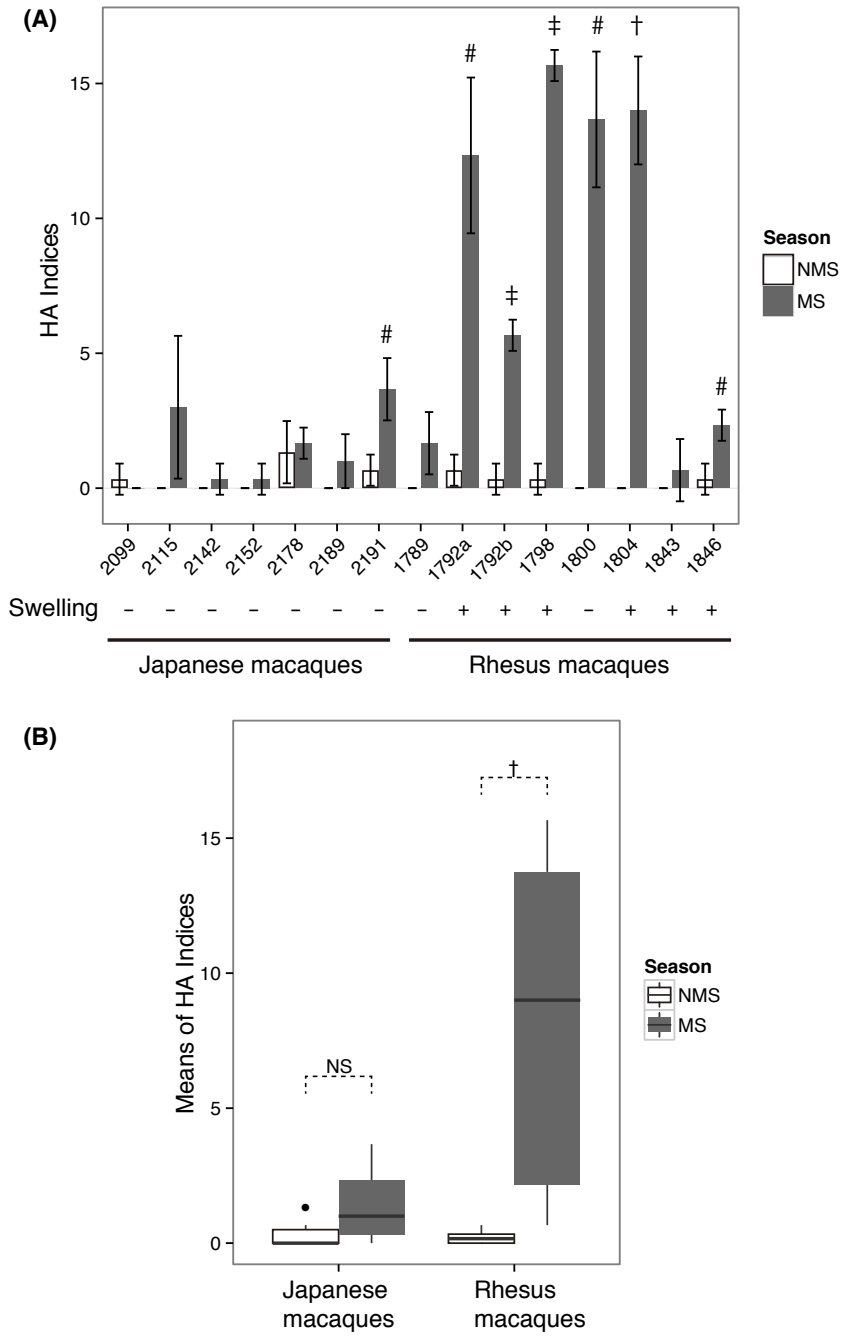

Figure 4.4 Seasonal changes in the HA indices of each specimen (A) and of species (B). Error bars indicate standard deviations in (A). The observed swelling status is represented by +/–signs. The description of box and whiskers plots in (B) is described in the legend for figure 3.5. # $p < 0.05$; † $p < 0.01$; ‡ $p < 0.001$; NS denotes not significant by t-test.

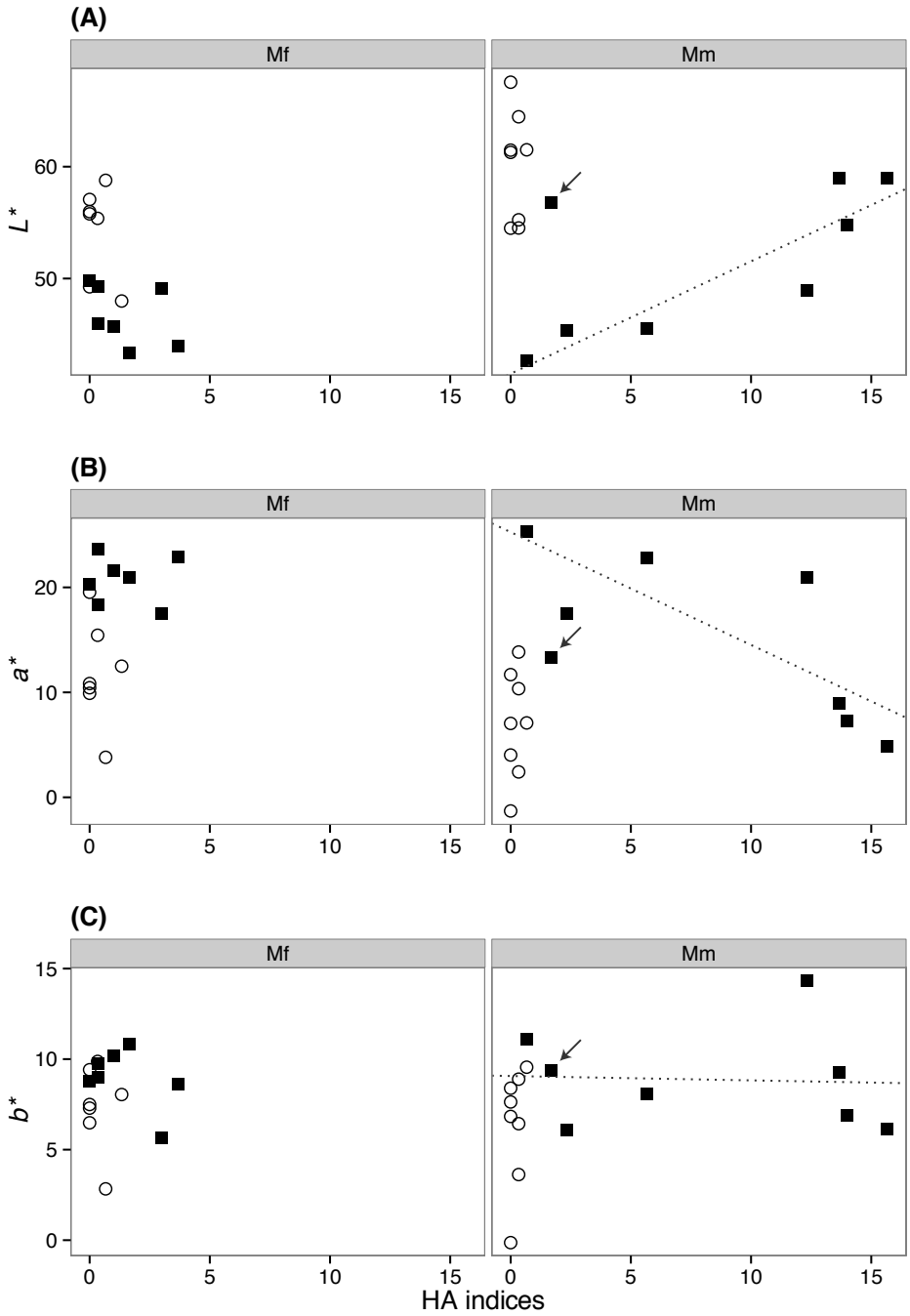

Figure 4.5 Relationships between HA indices and color variables. Blank circles indicate NMS; squares indicate MS. Dotted lines indicate regression lines of the rhesus macaques in MS excluding an outlier that is indicated by the arrow. Mf: Japanese macaques; Mm: rhesus macaques.

Chapter 5 Effects of steroid hormones on sexual skin coloration and expression of hormonal receptors

5.1 Introduction

In the previous chapters, I revealed that vascular functions, such as vasodilation and vascularization, and an increase of HA can affect seasonal sexual skin coloration. There is a consensus that sexual skin is under regulation of sex steroid hormones, such as estrogen and progesterone [Baulu, 1976; Carlisle et al., 1981]. In addition, it has been reported that estradiol (E2) induces sexual skin swelling and progesterone (P) restores the swelling during the menstrual cycle in ovariectomized pig-tailed macaques (*Macaca nemestrina*) [Carlisle, et al., 1981]. Therefore, estrogen and progesterone are postulated to operate through positive–negative feedback mechanisms in sexual skin.

Estrogen and progesterone act through their respective receptors, estrogen receptor (ER) and progesterone receptor (PR). ER and PR have many roles in reproductive functions in primates [Pelletier, 2000; Critchley et al., 2001; Cheng et al., 2005]. ER consists of ERα and ERβ. Until recently, ERβ was not fully understood with respect to its role in sexual skin, and therefore, the previous studies in the 1980s have focused only on classic ER (ERα) [Mosselman et al., 1996]. Although Bentley has shown localization of classic ER in the hindquarters of pig-tailed macaques, the localization around capillaries has not been found [Bentley et al., 1986]. Furthermore, although Onouchi and Kato have shown the existence of classic ER and PR with

biochemical methods in the hindquarter of Japanese macaques, they have not obtained histological information relating to the location of receptors [Onouchi & Kato, 1983]. In addition, previous reports have not examined the seasonal changes of these steroid receptors. Therefore, it is unknown whether ER/PR can regulate the cutaneous factors associated with seasonal sexual skin coloration. If ER/PR does not influence the factors through lack of its expression, the factors may not reflect hormonal conditions, e.g., ovulation. Such cutaneous factors investigated in the previous chapters include vascular endothelial cells and pericytes, which are believed to mediate vascular functions [Knowlton and Lee, 2012], and fibroblasts that produce hyaluronan with estrogen [Bentley et al., 1971; Bentley et al., 1986]. It is important to clarify how each cutaneous factor is influenced by the hormone receptors to improve understanding about the hormonal regulation of sexual skin coloration.

The hindquarter was the reddest, and a remarkable level of vascularization and vasodilation was found even during NMS among skin regions, when the cyclical hormonal surge was absent (figure 3.4). Therefore, I initially examined relationships between hormone, cutaneous factors, and skin color in the hindquarter during NMS. Secondly, four skin regions were investigated to demonstrate characteristics of localization of the hormone receptors; ERα, ERβ, and PR. Third, seasonal changes in the number of cells expressing ERα were examined to clarify which receptors can affect the cutaneous factors of seasonal skin coloration.

5.2 Materials and Methods

5.2.1 Subjects

This chapter consists of three sets of experiments. First, for the hormonal assay, three Japanese macaques aged 5 years (Mf2178, Mf2189, and Mf2191), and three rhesus macaques aged 4 years (Mm1843, Mm1846, and Mm1852) were recruited. Blood samples were collected from these animals twice a week, and color profiles were measured in the forehead (referred to as the face), median dorsum (referred to as the back), and 2–3 cm below the ischial callosity of each side (referred to as the hindquarter) once a week from August to September 2012. Second, for region comparison of hormone receptors, a Japanese macaque aged 21 years (Mf1481) and a rhesus macaque aged 4 years (Mm1915) were used. Biopsies were conducted in four skin regions: the face, abdomen, back, and hindquarter as described in Chapter 3 in July for Mf1481 and August for Mm1915 2014 (Fig. 3.1). Third, for seasonal comparison of the number of cells expressing ERα, four Japanese macaques aged 4–5 years (Mf2120, Mf2121, Mf2165, and Mf2189) and four rhesus macaques aged 3–4 years (Mm1789, Mm1792, Mm1843, and Mm1846) were sampled in August (NMS) and December (MS) 2011.

5.2.2 Hormonal assay

Blood samples (3 ml) were collected in tubes with heparin on the day of color measurements. Plasma was harvested by centrifugation at 3,000 × g for 20 min at 4°C,

and stored at −80°C for later analysis of hormone concentrations. Samples were extracted with diethyl ether and measured for concentrations of plasma estradiol. The concentrations of E2 and P were assessed by enzyme immunoassay (EIA) using commercially available kits for 17ß-estradiol (E2) determination (Estradiol EIA Kit, Catalog No. 582251: Cayman Chemical Company, Ann Arbor, MI, USA) and progesterone EIA Kit (Catalog No. 582601: Cayman Chemical Company). According to the manufacturer, cross-reactivities of the antibody for estrogen were 100% for 17ß-estradiol, 14% for estradiol-3-glucuronide, 12% for estrone, 10% for estradiol-17-glucuronide, and less than 1% for estriol, progesterone, and testosterone. Cross-reactivities of antibody for progesterone were 100% for progesterone, 14% for pregnenolone, and 7.2% for 17ß-estradiol. 17ß-estradiol and progesterone were measured in duplicate, following the instructions from the supplier. In brief, 50 µl of each sample extract was added to 100 µl of enzyme conjugate to each well in the plate. After incubation, the plates were washed and Ellman's reagent was added. The samples were measured at a wavelength of 450 nm on an automated microplate reader (GENios: TECAN, Zürich, Switzerland). The mean intra-assay coefficient of variation was 27.3% (n = 58) for the estrogen assay and 5.81% (n = 58) for the progesterone assay, and the mean inter-assay coefficient of variation was 24.2% (n = 3) for the estrogen assay and 20.0% (n = 3) for the progesterone assay.

5.2.3 Immunohistochemistry of hormone receptors

The anti-ERα antibody was a mouse monoclonal (clone 6F11), obtained from

Leica Biosystems (Cat. No. CL-ER-6F11, Wetzlar, Germany). The anti-ERβ antibody was a rabbit polyclonal (the immunogen is a synthetic peptide corresponding to residues A(55) E P Q K S P W C E A R S L E H(70) of rat ERβ), obtained from Thermo Scientific (Cat. No. PA1-311 Thermo Fisher Scientific, Inc., MA, USA). Both anti-ERα and anti-ERβ antibodies were used for Japanese macaques in a previous report [Takahashi et al., 2004]. The anti-PR antibody was a mouse monoclonal (clone hPRa 7), obtained from Thermo Scientific (Cat. No. MS-197). The anti-PR antibody was used for human skin [Kariya et al., 2005] and has species reactivity for monkey.

Paraffin sections (4 μm) were de-waxed in xylene and rehydrated through graduated ethanol to water. Antigens were retrieved through an antigen activation liquid for 20 min, autoclaved at 121°C (Buffer from Pathology Institute, code KN-09001). The following procedures were performed using the manual of DakoCytomation LSAB2 System-HRP (K0675, Agilent Technologies, CA, USA). In brief, endogenous biotin was blocked by incubation with DakoCytomation Biotin-Blocking System (Code X0590). Endogenous peroxidase was blocked by incubation for 5 minutes with Dako REAL™ Peroxidase-Blocking Solution (Code S2023). Antibodies were individually diluted in TBS containing 1% BSA. Dilutions for antibodies were 1:200 for ERα; 1:200 for ERβ, and 1:200 for PR. Sections were incubated with antibodies overnight at 4°C. For negative controls, the primary antibodies were replaced with TBS alone. Before and after the incubation of the secondary antibody, sections were rinsed in TBS. Sections were incubated in BIOTINYLATED LINK solution for 10 minutes at room temperature. The sections were incubated in STREPTAVIDIN-HRP solution for 10 minutes at room

temperature. After thorough washing in TBS, sections were developed with DAB CHROMOGEN in DAB SUBSTRATE BUFFER, slightly counterstained with hematoxylin, and dehydrated through an ethanol series, followed by exposure to xylene and mounting.

5.2.4 Image Analysis

Captured regions were randomly selected in the sub-epidermal area in sections of sexual skin. Five images were captured using a light microscope with a Leica system (Leica CTR 6000) for each subject. All images were stored at about 6400 × 5700-pixelated digital files, giving a pixel resolution of about 0.23 μm. The number of cells expressing ERα and cells not expressing ERα (approximately 500 cells for each sample) was manually counted in the acquired five images using Adobe Photoshop CS5. Additionally, to investigate relationship between pericyte and vascular factors, ten vascular capillaries were randomly selected in the sections of each specimen, then the numbers of pericytes expressing ERα and pericytes not expressing ERα were manually counted.

5.2.5 Data analysis

As for the monthly analysis of three Japanese and three rhesus macaques, the range of a^* was calculated as the difference of the maximum value and the minimum value in each specimen. The Pearson's correlation coefficients were calculated for the a^* variables and the indices of vascular factors; capillary density and size. The different

ratios of cells expressing ERα between the skin regions were tested with Welch's two-sample t-test. As for the seasonal analysis of ERα, the ratio of positively stained cells or pericytes was calculated for each specimen. The Pearson's correlation coefficients assessed the ratio of cells or pericytes expressing ERα and the capillary density, size, or a^* variable were calculated. A p value of less than 0.05 was considered significant.

5.3 Results

As for monthly analysis of the four skin regions using three Japanese and three rhesus macaques, the average ± SD of the ranges of a^* was 0.77 ± 0.42 for the back, 1.67 ± 0.31 for the face, and 5.73 ± 2.96 for the hindquarter in the Japanese macaques, whereas it was 1.13 ± 0.85 for the back, 1.33 ± 0.70 for the face, and 5.63 ± 0.49 for the hindquarter in the rhesus macaques. Over a month, the variable a^* changed in the hindquarter in both Japanese and rhesus macaques (figure 5.1). The fluctuation of a^* in the hindquarter correlated with the capillary size ($r = 0.46$, $t = 2.41$, $df = 22$, $p < 0.05$), but not the capillary density ($r = 0.04$, $t = 0.20$, $df = 22$, $p > 0.05$) when data of all specimens were combined. In addition, the fluctuation of a^* in the hindquarter did not significantly correlate with plasma concentration of E2 or P (E2: $r = 0.40$, $t = 2.07$, $df = 22$, $p = 0.050$; P: $r = -0.32$, $t = -1.58$, $df = 22$, $p = 0.12$; figure 5.2). A significant correlation was found between the plasma level of P and capillary size ($r = -0.56$, $t = -3.21$, $df = 22$, $p < 0.01$), whereas no significant correlation was found between

hormones and capillary density (table 5.1).

ERα was expressed in the hindquarter area more than in any other skin regions according to microscopic observation (figure 5.3). ERβ and PR were homogenously expressed in all skin regions; the hindquarter, face, back, and abdomen, in both species. The average ± SD of ratio of cells expressing ERα in the abdomen, back, face, hindquarter was 0.073 ± 0.045, 0.012 ± 0.025, 0.065 ± 0.045, 0.15 ± 0.054, respectively, in the Japanese macaques, and 0.15 ± 0.13, 0.34 ± 0.075, 0.49 ± 0.070, and 0.71 ± 0.075, respectively in the rhesus macaques (figure 5.4). The ratio of cells expressing ERα was the highest in the hindquarter in both Japanese and rhesus macaques (t value between hindquarter and face in Mf: $t = 2.55$, $df = 7.79$, $p < 0.05$; between hindquarter and face in Mm: $t = 4.40$, $df = 7.98$, $p < 0.01$ by Welch's two-sample t-test). ERα was highly expressed in the pericytes and fibroblasts but was slightly expressed in the endothelial cells (figure 5.5).

As for seasonal analyses of ERα in hindquarter skin, the average of ratio of cells expressing ERα ± SD in the Mf2120, Mf2121, Mf2165, Mf2189, Mm1789, Mm1792, Mm1843, and Mm1846 was 0.35 ± 0.031, 0.19 ± 0.063, 0.45 ± 0.064, 0.40 ± 0.036, 0.28 ± 0.024, 0.38 ± 0.034, 0.47 ± 0.034, and 0.36 ± 0.048, respectively, in NMS, and 0.49 ± 0.045, 0.61 ± 0.029, 0.45 ± 0.064, 0.47 ± 0.020, 0.54 ± 0.035, 0.46 ± 0.032, 0.49 ± 0.040, and 0.50 ± 0.043, respectively, in MS (figure 5.7). The expression of ERα increased during NMS into MS in both Japanese and rhesus macaques (figure 5.6 and 5.7). The ratio of cells expressing ERα correlated with the capillary size and a^* (correlation coefficient between ERα and capillary size: $r = 0.62$, $df = 14$, $p < 0.05$;

between ERα and *a**: r = 0.70, df = 14, $p < 0.01$), but not with the capillary density (figure 5.8). The ratio of pericytes expressing ERα correlated with the capillary size (r = 0.72, t = 3.90, df = 14, $p < 0.01$) and *a** (r = 0.77, t = 4.46, df = 14, $p < 0.001$) in four Japanese and four rhesus macaques. When the correlations between the ratio and capillary size were tested in each species, significant correlation was found in the rhesus macaques (r = 0.95, t = 7.15, df = 6, $p < 0.001$). Additionally, the ratio correlated with *a** in both the Japanese (r = 0.74, t = 2.70, df = 6, $p < 0.05$) and the rhesus macaques (r = 0.80, t = 3.26, df = 6, $p < 0.05$).

5.4 Discussion

The skin tissues of three Japanese and three rhesus macaques during NMS were examined to investigate the relationship between skin color, steroid hormones and vascular factors. The *a** variable of the hindquarter fluctuated over a month during NMS (figure 5.1), and the fluctuation of *a** was associated with the capillary size but not with the capillary density. This suggests that vasodilation/vasoconstriction rather than vascularization changed the sexual skin color during the observation period even during NMS. Although the correlation coefficients between *a** and hormonal levels were not significant, the coefficient between E2 and *a** was positive, whereas the coefficient between P and *a** was negative. It was reported that treatment of P in the ovariectomized pig-tailed macaques resulted in a decrease in vascular lumen size and sexual skin color [Carlisle, et al., 1981]. Similarly, P was negatively associated with the

capillary size but not with the capillary density in this study. The plasma level of P during NMS (approximately 1,000 pg/ml) was lower than the peak level during menstrual cycles (approximately 6,000 pg/ml) reported in a previous study [Czaja et al., 1977]. The results suggest that an increase in P at low levels leads to vasoconstriction resulting in a decrease in sexual skin redness. It could be also suggested that vascular lumen size can be easily fluctuated depending on sex hormones at low levels, which supports the suggestion that vasodilation/vasoconstriction is a comparatively short-term factor for skin coloration.

ERα, not ERβ and PR, was expressed more conspicuously in the hindquarter than in other skin regions in the Japanese macaque (Mf1481) and the rhesus macaque (Mm1915) during NMS (figure 5.3 and 5.4). The ratios of cells expressing ERα were consistently higher in Mm1915 aged 4 years than in Mf1481 aged 21 years. The reduction of ovarian function occurs at around 20-25 years in Japanese and rhesus macaques [Takahata, et al., 1995; Walker, 1995; Gilardi, et al., 1997; Nicolas, et al., 2005]. Additionally, there was no species difference in the level of ERα expression in figure 5.7, thus the difference in the ratio may be due to the older age of Mf1481 compared with Mm1915. A previous biochemical study suggested that classic ER (ERα) existed in the hindquarters but not in abdomens in chimpanzees [Ozasa and Gould, 1982]. In this study, the varied expression of ERα between the four skin regions suggested that ERα play particular roles for each skin region. It was also reported that the concentration of nuclear classic ER elevated with a degree of swelling in chimpanzees [Ozasa and Gould, 1982], which suggested that ERα mediated sexual skin

changes. ERα may mainly produce the characteristic sexual skin changes in hindquarters also in macaques.

Capillary pericytes are believed to regulate vasodilation/vasoconstriction as well as vascular smooth muscle cells [Lamalice et al., 2007; reviewed in Hamilton et al., 2010], whereas fibroblasts produce hyaluronan in skin with E2 [Sobel, 1965, Bentley et al., 1986]. In this study, the expression of ERα was found in a small number of vascular endothelial cells and in large number of capillary pericytes and fibroblasts (figure 5.5 and figure 5.6), and the ratio of cells expressing ERα of all cell types in the sub-epidermal area was increased from NMS to MS (figure 5.7). When only pericytes were considered, the ratio of pericytes expressing ERα correlated with a^* and the capillary size, but did not with the capillary density in four Japanese and four rhesus macaques (figure 5.8). Therefore, ERα may regulate seasonal vasodilation and HA synthesis. However, when the data were separated into each species, the ratio correlated with the capillary size and a^* only in four rhesus macaques. In contrast, the ratio did not correlate with capillary size but did correlate with a^* in four Japanese macaques. Although ERα may regulate skin redness also in Japanese macaques, it is possible that there are other mechanisms than vasodilation. For example, oxidation/deoxidation of hemoglobin modify skin redness in human [Changizi et al., 2006], but it is still unknown that sex hormones can regulate oxidation of hemoglobin. The Japanese macaques exhibited redder and darker sexual skin (Chapter 2) and enlarged capillaries (Chapter 3) even in NMS, which may indicate that non-hormonal regulations of vascular functions exist in them.

ERβ and PR were expressed in endothelial cells as well as pericytes and fibroblasts in both species. Mediation of not only pericytes but also endothelial cells is required for vascularization [Lamalice et al., 2007]. Although more detail studies using cultured vascular cells are required, it might be possible that ERβ and/or PR are involved in vascularization. In conclusion, seasonal coloration of hindquarters may be because of vasodilation mainly regulated by pericytes expressing ERα at least in the rhesus macaques. In addition, fibroblasts expressing ERα may produce HA in the rhesus macaques. The species difference in seasonal coloration mechanisms found in Chapter 3 and 4 may result from differences in the degree of gene transcriptions activated by hormonal receptors. The basis of gene regulation may be shared in the closely related macaque species. Experiments that use cultural vascular-related cells from sexual skin will examine these implications.

Table 5.1

Correlation coefficients between plasma hormone levels and capillaries in three Japanese macaques and three rhesus macaques.

	CAPILLARY DENSITY (counts/μm^2)	CAPILLARY SIZE (Log, μm^2)
E2	0.05	−0.031
P	0.30	−0.56†

† $p < 0.01$

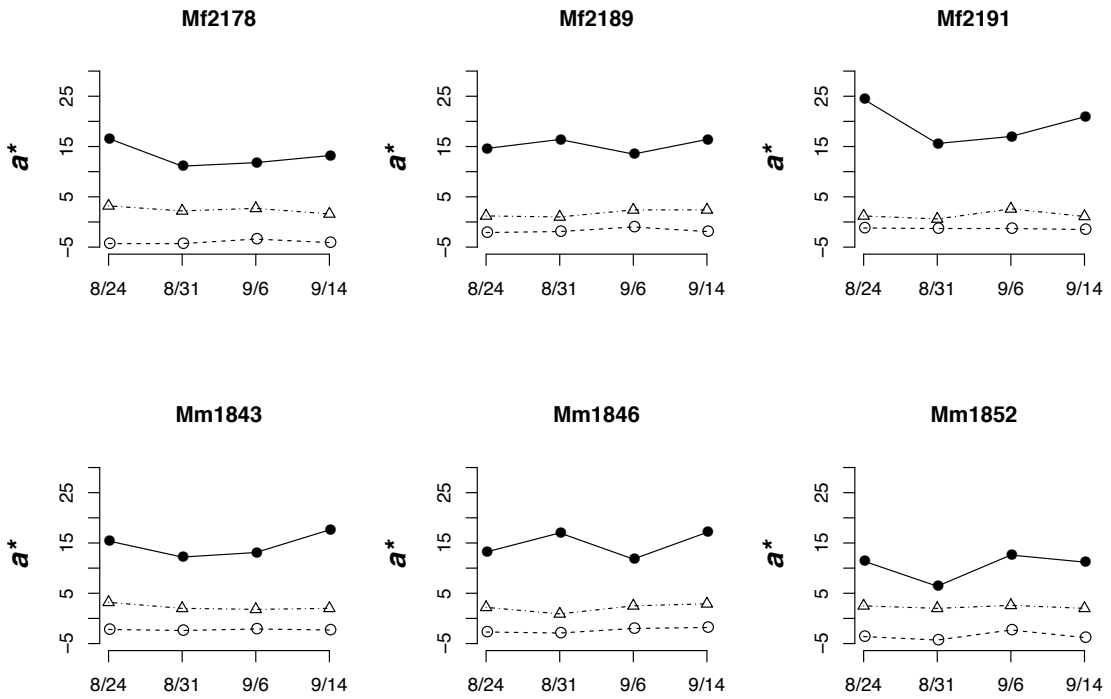

Figure 5.1 Fluctuation of mean *a** in three Japanese macaques and three rhesus macaques used for the hormonal assay between 24 Aug and 14 Sep, 2012. Standard deviations of measured color data were so small and not shown in the figures. ●: Hindquarter; ○: Back; △: Face.

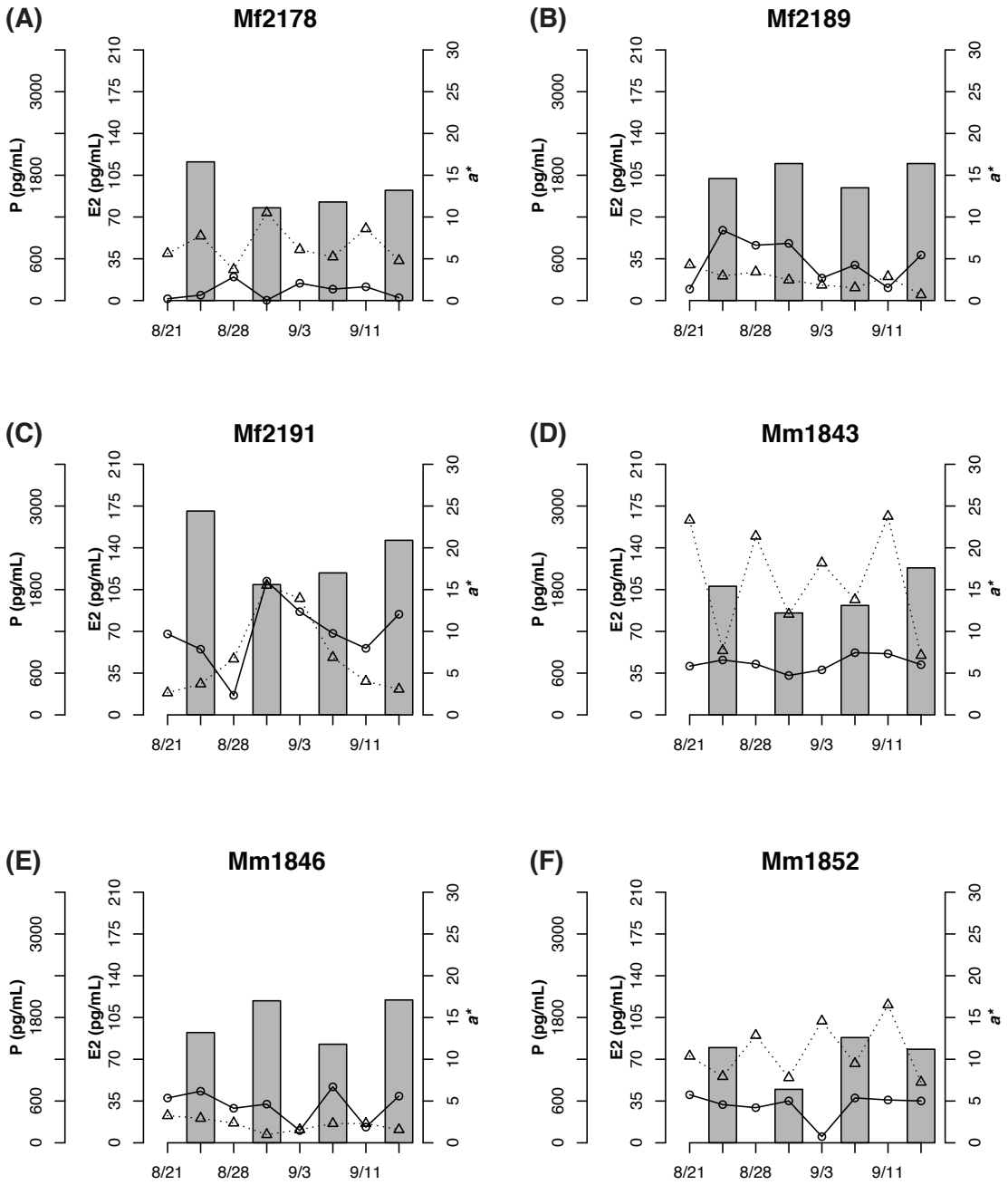

Figure 5.2 Fluctuation of *a** (bars) and plasma hormone levels; estradiol (-O-), and progesterone (-△-).

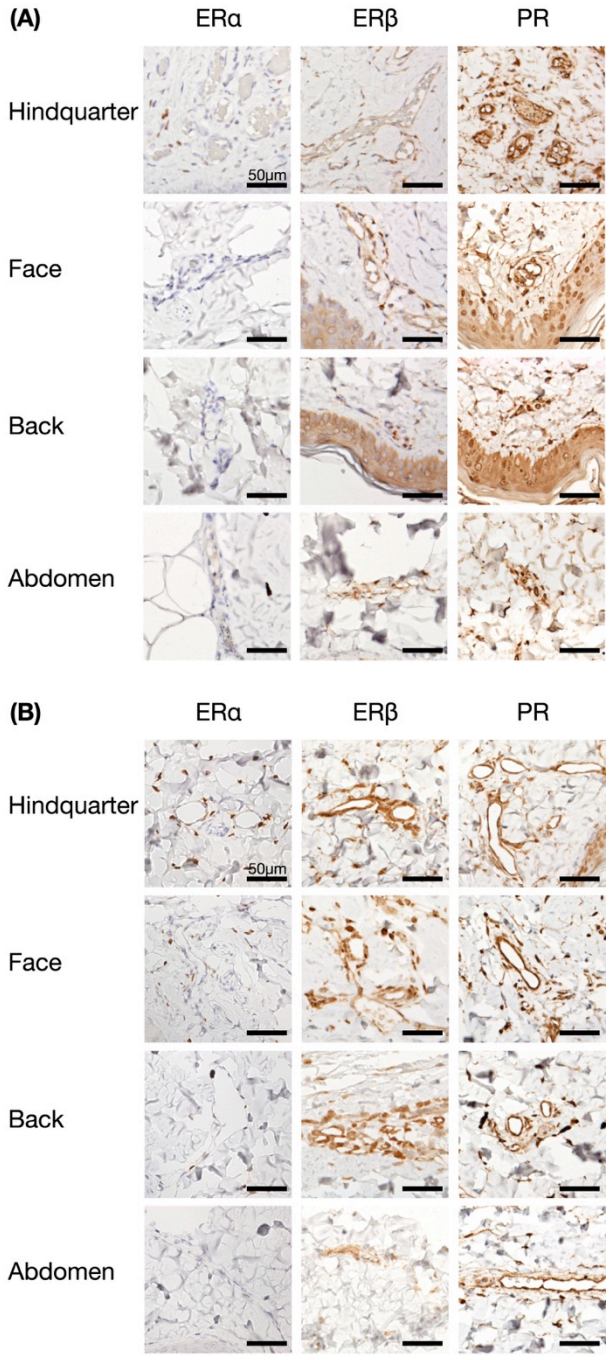

Figure 5.3 Localization of ERα, ERβ, and PR by immunohistochemistry in four skin regions from a Japanese macaque (Mf1481) (A) and a rhesus macaque (Mm1915) (B). Bar, 50 μm.

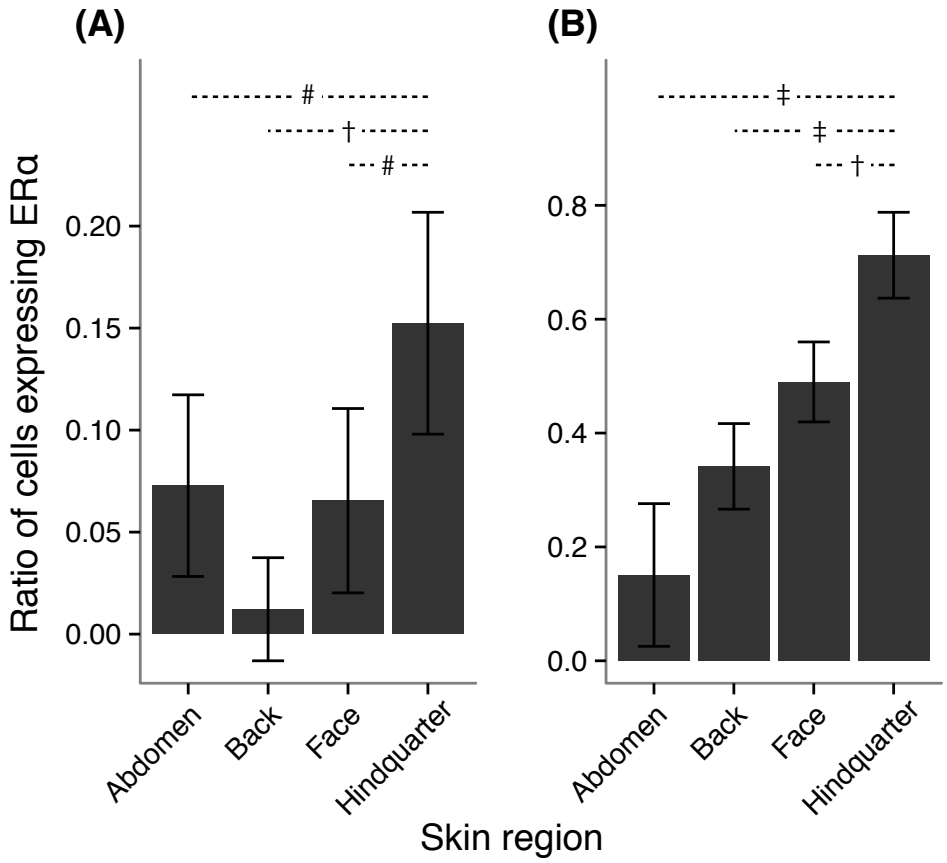

Figure 5.4 Mean ratio of cells expressing ERα in four skin regions from a Japanese macaque (Mf1481) (A) and a rhesus macaque (Mm1915) (B). Error bars indicate standard deviations. # $p < 0.05$; † $p < 0.01$; ‡ $p < 0.001$ by Welch's two-sample t-test.

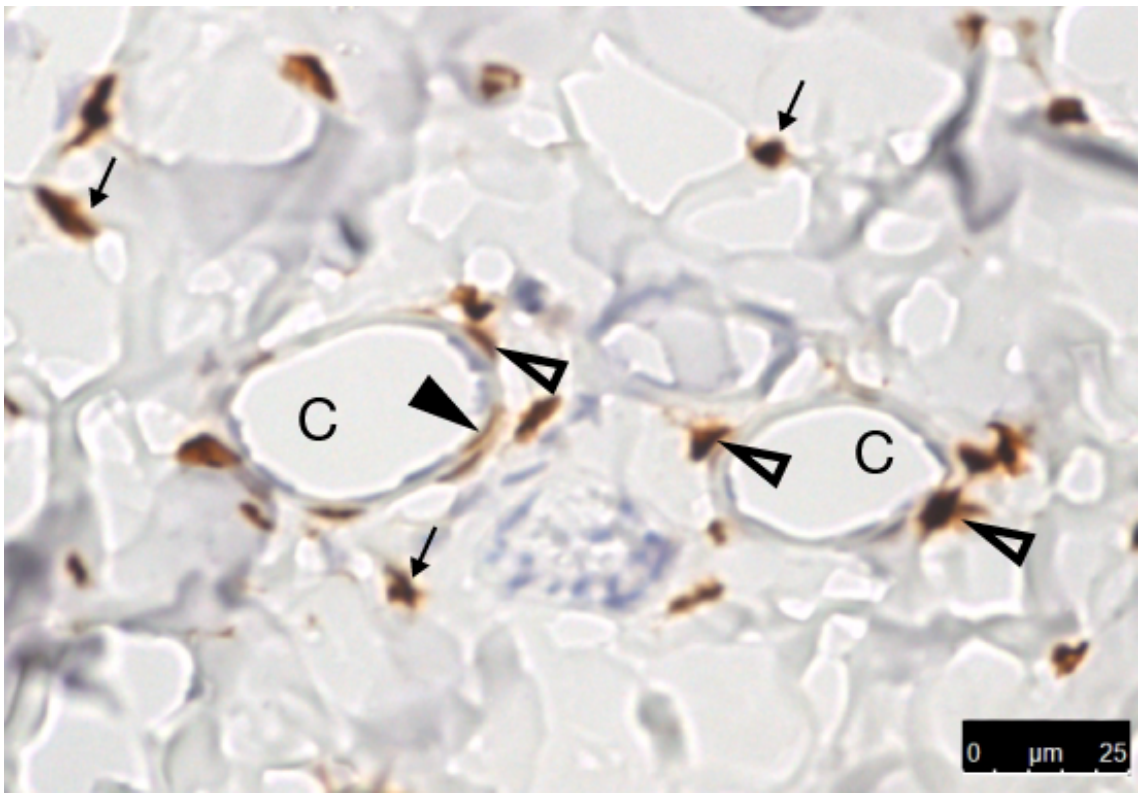

Figure 5.5 Localization of ERα in the hindquarter of a rhesus macaque (Mm1915). Bar, 25 µm.

◀ : vascular endothelial cell

◁ : pericyte (perivascular cell)

← : fibroblast

"C" : vascular capillary

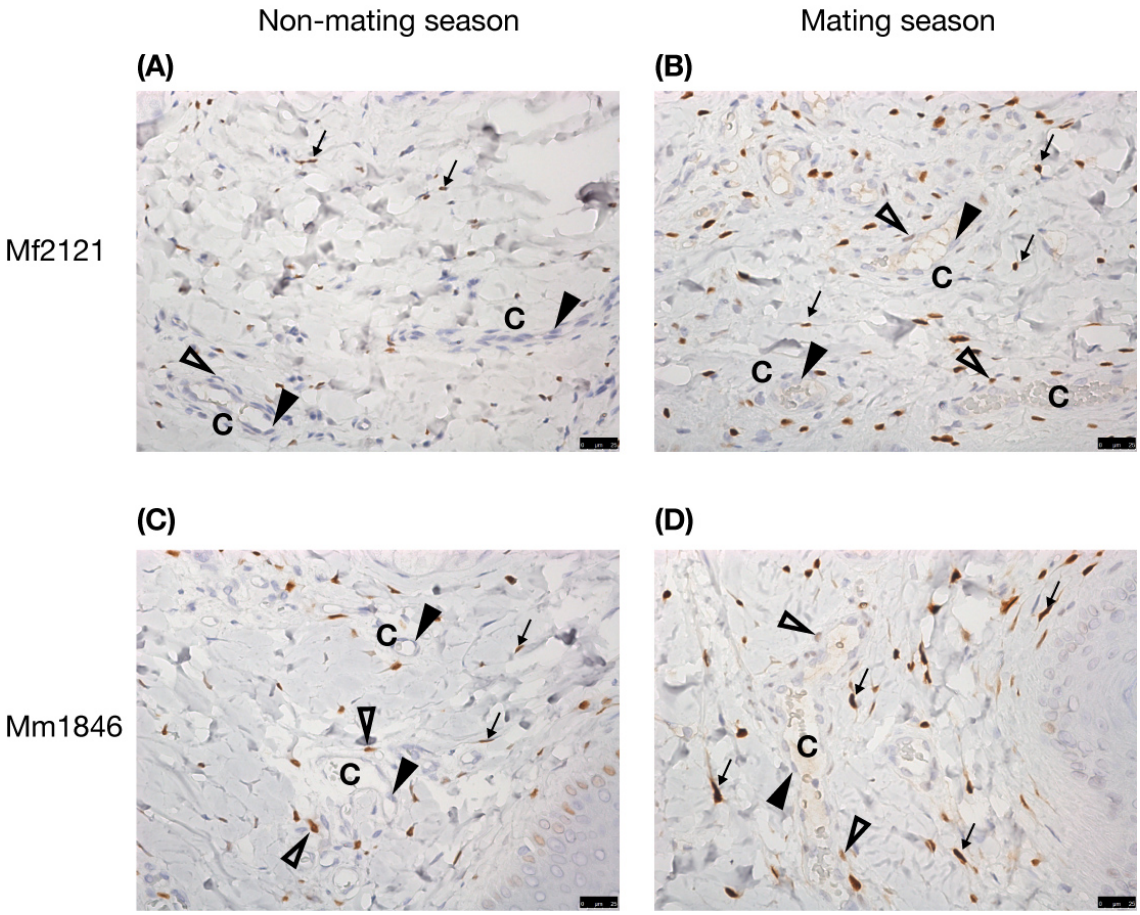

Figure 5.6 Localization of ERα in the hindquarter of the Japanese macaque and the rhesus macaque. Bar, 25 µm.

◀ : vascular endothelial cell

◁ : pericyte (perivascular cell)

← : fibroblast

"C" : vascular capillary

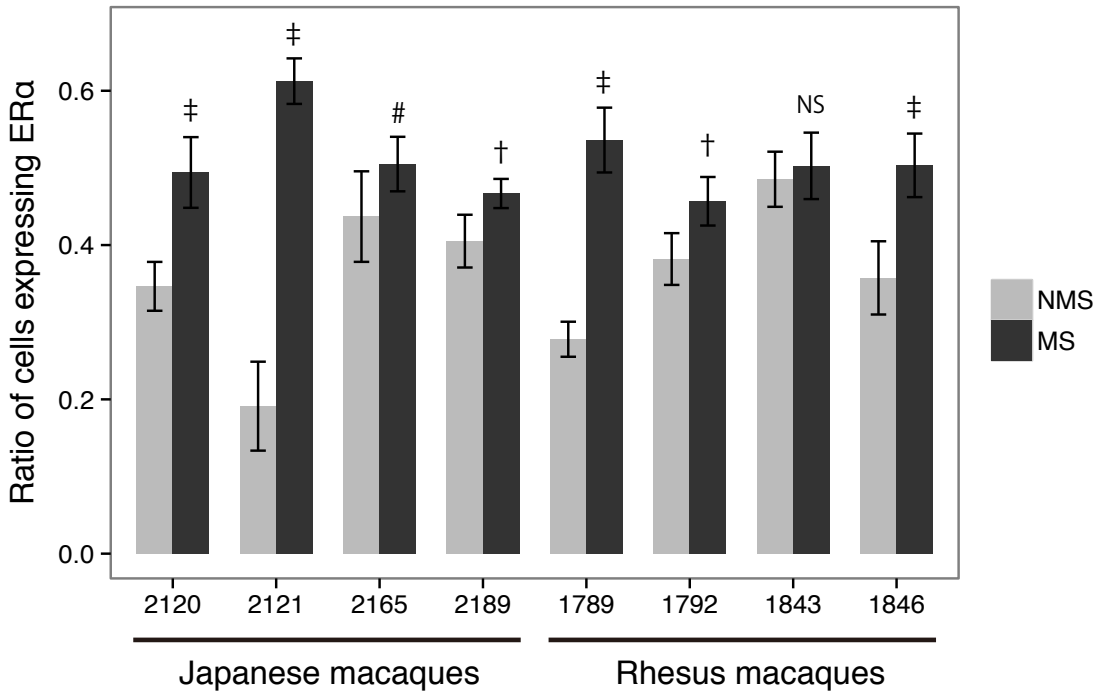

Figure 5.7 Seasonal changes in the mean ratio of cells expressing ERα. Error bars indicate standard deviations. # $p < 0.05$; † $p < 0.01$; ‡ $p < 0.001$; NS denotes not significant by Welch's two-sample t-test.

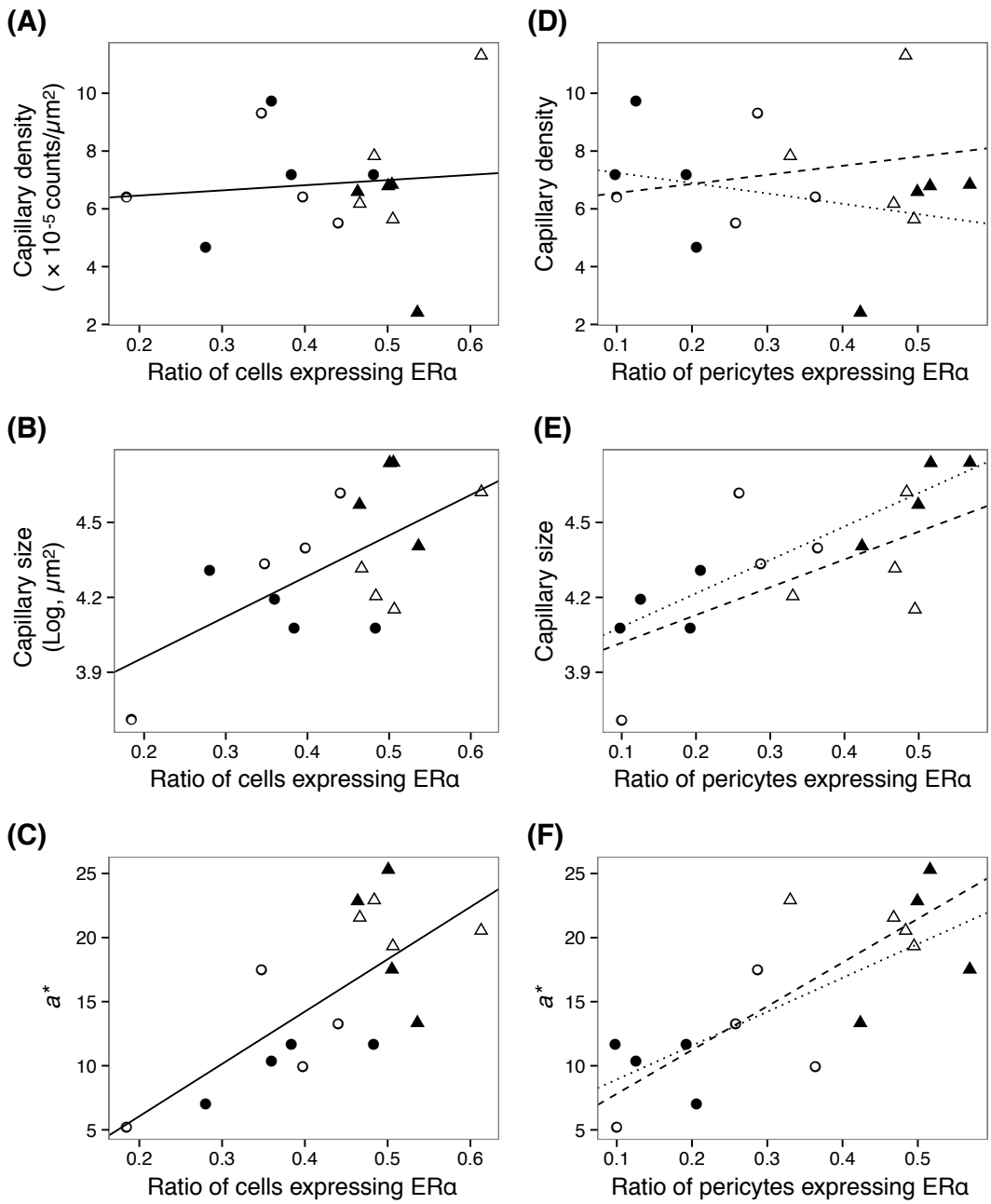

Figure 5.8 Relationships between the ratio of cells or pericytes expressing ERα and vascular factors or skin redness. Lines indicate regression lines as shown in the following examples.

——— : all specimens (four Japanese and four rhesus macaques)

------- : four Japanese macaques

····· : four rhesus macaques

○: Mf in NMS; △: Mf in MS; ●: Mm in NMS; ▲: Mm in MS.

Chapter 6 Conclusion

This study revealed common and different aspects of sexual skin transformation between Japanese and rhesus macaques. Both species shared similar seasonal coloration in their hindquarters; the sexual skin became redder, darker, and yellower from the NMS to the MS. The coloration was mainly subjected by vasodilation, which may be mediated by vascular pericytes expressing ERα. This is the first study that demonstrates the common mechanism of sexual skin coloration in the macaques.

It is noticed that the two macaque species have different coloration. Japanese macaques exhibited redder and darker sexual skin both during NMS and MS, which suggests different mechanisms of skin coloration between the two macaque species. Vascularization was found only in the Japanese macaques. Furthermore, dermal melanin content was more abundant in the Japanese macaques than in the rhesus macaques. The level of vascularization and abundant melanin made the sexual skin redder and darker in the Japanese macaques, which resulted in species differences in coloration both during the NMS and the MS. Moreover, vascularization and abundant melanin are relatively long-term responses to vasodilation/vasoconstriction; therefore, the effects of those robust factors may not greatly fluctuate through the MS and will raise redness and darkness. The short-term and long-term mediations of coloration might generate broad color signals in the Japanese macaques.

As for sexual swelling, the sexual skin of rhesus macaques was affected by an increase in hyaluronan, resulting in a loss of redness and darkness in sexual skin. An

increase in hyaluronan leads to sexual swelling as the long-term response, which counteracts skin coloration through vasodilation in rhesus macaques. The Japanese macaques experience a redder and darker sexual skin by vascularization and melanin, whereas the rhesus macaques lose the redder and darker sexual skin through increased HA. These results can explain the species differences in sexual skin redness and darkness between the two macaque species.

Although there were similar and distinct coloration mechanisms found in the Japanese and rhesus macaques, the localization of estrogen and progesterone receptors were qualitatively same. This suggests that the closely related macaques share most gene regulations for coloration and swelling of sexual skin. As for vascular factors, vasodilation and vascularization usually work together in mediating skin redness in primates. Even if vascularization increases the number of vascular capillaries, swelling can counteract the increase in capillary density in the rhesus macaques. As for HA synthesis, a Japanese macaques showed a significant increase in HA from NMS to MS. The species differences relating to these factors might result from the difference in degrees of gene regulation shared by the two macaque species. However, it should be noted that the level of difference could affect apparent cues for fertility detected by the males.

In this thesis, I have demonstrated histologically that vasodilation was the main mechanism for seasonal sexual skin coloration, whereas other factors, such as vascularization, melanin, and hyaluronan caused differences in the coloration between closely related macaques (table 6.1). As for insights into function of obscured ovulation,

the short-term vasodilation according to internal sex hormone levels may play a major role in coloration. In addition, long-term vascularization and abundant melanin may promote coloration in Japanese macaques, whereas long-term increase in HA level may reduce coloration in rhesus macaques. However, the results of this study should be considered as indirect demonstrations based on the correlation analyses. Behavioral analyses considering both size and color of sexual skin will reveal whether such combined cues play roles in mate-choice and determining paternity confusion or not. In addition, future studies using non-invasive methods to detect skin coloration, vascular dynamics, and sexual hormone levels and studies using cultured cells from hindquarter skin will elucidate the direct mechanisms of hormonal regulation in influencing factors of sexual skin transformations. The major mechanisms of the transformations found in this study can help to understand the effect of sexual skin on breeding behavior in primates. Additionally, the species comparison of these mechanisms will provide evolutionary insight into the mechanism of sexual skin development in primates.

Table 6.1

Findings from this thesis

Morphological level	Quantitative evaluation with spectocolorimetry of seasonal skin coloration revealed; ● similar skin coloration in Japanese and rhesus macaques; ➢ lightness ↓, redness ↑, and yellowness ↑, ● darker and redder sexual skin in Japanese macaques.
Histological level	Quantitative evaluation with microscopic and digital image analyses revealed; ● the main mechanism for sexual skin coloration; ➢ vasodilation in both Japanese and rhesus macaques: redness ↑ and lightness ↓, ● secondary mechanisms modified sexual skin coloration in each macaque species; ➢ vascularization and rich melanin in the Japanese macaques: redness ↑ and lightness ↓, ➢ hyaluronan increasing in the rhesus macaques: redness ↓ and lightness ↑.
Molecular level	Increased number of vascular pericytes expressing ERα may promote vasodilation, resulting in seasonal sexual skin coloration.

Acknowledgements

I would like to express my sincere gratitude to all the people who helped me in writing this PhD thesis. A lot of people have kindly helped me and given me salient advice.

My heartfelt appreciation goes to Professor Takafumi Ishida whose comments and suggestions were incredibly valuable throughout the course of my study. Without his exact supervision I could not have completed this thesis.

I would like to express my sincere gratitude to Associate Professor Juri Suzuki, who helped me in sampling specimens at the Primate Research Institute, Kyoto University. I am grateful to Professor Kenichi Aoki, Department of Biological Sciences, University of Tokyo for his generous permission in using the spectrocolorimeter. I also thank Professor Roscoe Stanyon for his comments on my study.

I thank all the members of the Unit of Human Biology and Genetics, The University of Tokyo, particularly, Dr. Kazunari Matsudaira, Chiaya Sakae, Gento Tadakara, and Marie Saitou for their help. I also thank Taro Yoshida for his great contribution to the statistical analyses.

I would also like to express my gratitude to my family for their moral support and warm encouragements, particularly my father Professor Ryo Ono who opened my eyes to academic research.

This work was supported by the Cooperation Research Program of Primate Research Institute, Kyoto University.

The responsibility of any errors within this thesis is of course my own.

References

Alaluf S, Atkins D, Barrett K, Blout M, Carter N, Heath A (2002). Ethnic variation in melanin content and composition in photoexposed and photoprotected human skin. Pigment Cell Research 15:112–118.

Alaluf S, Atkins D, Barrett K, Blount M, Carter N, Heath A (2002). The Impact of epidermal melanin on objective measurements of human skin colour. Pigment Cell Research 15: 119–126.

Anderson CM, Bielert CF (1994). Adolescent exaggeration in female catarrhine primates. Primates 35: 283–300.

Baulu J (1976). Seasonal sex skin coloration and hormonal fluctuations in free-ranging and captive monkeys. Hormones and Behavior 7: 481–494.

Bowmaker JK, Dartnall HJ, Lythgoe JN, Mollon JD (1978). The visual pigments of rods and cones in the rhesus monkey, Macaca mulatta. Journal of Physiology 274: 329–348.

Bradley BJ, Mundy NI (2008). The primate palette: The evolution of primate coloration. Evolutionary Anthropology: Issues, News, and Reviews 17: 97–111.

Brandon-Jones D, Eudey AA, Geissmann T, Groves CP, Melnick DJ, Morales JC, Shekelle M, Stewart CB (2004). Asian primate classification. International Journal of Primatology 25: 97–164.

Cerda-Molina AL, Hernández-López L, Chavira R, Cárdenas M, Paez-Poncea D, Cervantes-De la Luza H, Mondragón-Ceballosa R. (2006). Endocrine changes in

male stumptailed macaques (*Macaca arctoides*) as a response to odor stimulation with vaginal secretions. Hormones and Behavior 49:81–7.

Changizi MA, Zhang Q, Shimojo S (2006). Bare skin, blood and the evolution of primate colour vision. Biology Letters 2: 217–21.

Chen Z, Yuhanna IS, Galcheva-Gargova Z, Karas RH, Mendelsohn ME, Shaul PW (1999). Estrogen receptor α mediates the nongenomic activation of endothelial nitric oxide synthase by estrogen. Journal of Clinical Investigation 103:401–406.

Cheng G, Li Y, Omoto Y, Wang Y, Berg T, Nord M, Vihko P, Warner M, Piao YS, Gustafsson JA (2005). Differential regulation of estrogen receptor (ER)α and ERβ in primate mammary gland. The Journal of Clinical Endocrinology & Metabolism 90:435–44.

Collings MR (1926). A study of the cutaneous reddening and swelling about the genitalia of the monkey, Macacus rhesus. The Anatomical Record 33: 271–287.

Costa F, Biaggioni I (1998). Role of Nitric Oxide in Adenosine-Induced Vasodilation in Humans. Hypertension 31:1061–1064.

Critchley HOD, Brenner RM, Teresa A. H, KarinW, Nihar RN, Slayden OD, Millar MR, Saunders PTK (2001). Estrogen Receptor beta, But Not Estrogen Receptor alpha, Is Present in the Vascular Endothelium of the Human and Nonhuman Primate Endometrium. The Journal of Clinical Endocrinology & Metabolism 86:1370–1378.

Czaja JA, Eisele SG, Goy RW (1975). Cyclical changes in the sexual skin of female rhesus: relationships to mating behavior and successful artificial insemination.

Primate Research pp: 83–92.

Deschner T, Heistermann M, Hodges K, zBoesch C (2004). Female sexual swelling size, timing of ovulation, and male behavior in wild West African chimpanzees. Hormones and Behavior 46:204–215.

Dixson A (1983). Observations on the evolution and behavioral significance of 'sexual skin' in female primates. In Advances in the Study of Behavior Vol. 13 (Rosenblatt JS, Hinde RA, Beer C, Busnel MC eds.), pp 63–106.

Dubuc C, Brent LJN, Accamando AK, Gerald MS, MacLarnon A, Semple S, Heistermann M, Engelhardt A (2009). Sexual skin color contains information about the timing of the fertile phase in free-ranging Macaca mulatta. International Journal of Primatology 30: 777–789.

Gerald MS, Waitt C, Little AC, Kraiselburd E (2007). Females pay attention to female secondary sexual color: an experimental study in Macaca mulatta. International Journal of Primatology 28: 1–7.

Gilardi KV (1997). Characterization of the onset of menopause in the rhesus macaque. Biology of Reproduction, 57(2), 335–340.

Hamada Y, Watanabe T, Iwamoto M (1992) Variation of Body Color within Macaques, Especially in the Japanese Macaques. Primate Research 8: 1-23.

Hamilton NB, Attwell D, Hall CN (2010). Pericyte-mediated regulation of capillary diameter: a component of neurovascular coupling in health and disease. Frontiers in Neuroenergetics

Higham JP, MacLarnon AM, Ross C, Heistermann M, Semple S (2008). Baboon sexual

swellings: information content of size and color. Hormones and Behavior 53: 452–462.

Higham JP, Brent LJN, Dubuc C, Accamando AK, Engelhardt A, Gerald MS, Heistermann M, Stevens M (2010). Color signal information content and the eye of the beholder: a case study in the rhesus macaque. Behavioral Ecology 21: 739–746.

Higham JP, Heistermann M, Saggau C, Agil, Muhammad PFD, Engelhardt A (2012). Sexual signalling in female crested macaques and the evolution of primate fertility signals. BMC Evolutionary Biology 12: 89.

Hirshburg J, Choi B, Nelson JS, Yeh AT (2006). Collagen solubility correlates with skin optical clearing. Journal of Biomedical Optics 11:040501.

Jablonski N, Chaplin G (2000). The evolution of human skin coloration. Journal of Human Evolution 39: 57–106.

Jablonski N (2004). The Evolution of Human Skin and Skin Color. Annual Review of Anthropology 33:585–623.

Jablonski N, Chaplin G (2010). Human skin pigmentation as an adaptation to UV radiation. Proceedings of the National Academy of Sciences of the United States of America 107: 8962–8968.

Jacobs GH, Deegan JF (1999). Uniformity of colour vision in Old World monkeys. Proceedings of the Royal Society B: Biological Sciences 266:2023–8.

Kariya Y, Moriya T, Suzuki T, Chiba M, Ishida K, Takeyama J, Endoh M, Watanabe M, Sasano H (2005). Sex Steroid Hormone Receptors in Human Skin Appendage and

its Neoplasms. Endocrine Journal 52:317–325.

Kurihara K, Nakanishi N, Ueha T (2000). Regulation of Na(+)-K(+)-ATPase by cAMP-dependent protein kinase anchored on membrane via its anchoring protein. American Journal of Physiology. Cell Physiology 279: C1516–1527.

Kwon-Chung KJ, Hill WB, Bennett JE (1981). New, special stain for histopathological diagnosis of cryptococcosis. Journal of Clinical Microbiology 13: 383–387.

Lamalice L, Le Boeuf F, Huot J (2007). Endothelial cell migration during angiogenesis. Circulation Research 100: 782–94.

Luksha L, Agewall S, Kublickiene K (2009). Endothelium-derived hyperpolarizing factor in vascular physiology and cardiovascular disease. Atherosclerosis 202: 330–244.

McLeod SD, Ranson M, Mason RS (1994). Effects of estrogens on human melanocytes in vitro. The Journal of Steroid Biochemistry and Molecular Biology 49: 9–14.

Moncada S, Higgs EA, Hodson F, Knowles RG, Lopez-Jaramillo P, McCall T, Palmer RMJ, Radomski MW, Rees DD, Schulz R (1991). The L-Arginine: Nitric Oxide Pathway. Journal of Cardiovascular Pharmacology 17: S1–S9.

Mori A, Yamaguchi N, Watanabe K, Shimizu K (1997). Sexual Maturation of Female Japanese Macaques Under Poor Nutritional Conditions and Food-Enhanced Perineal Swelling in the Koshima Troop. International Journal of Primatology 18: 553–579.

Mosselman S, Polman J, Dijkema R (1996). ERβ: Identification and characterization of a novel human estrogen receptor. FEBS Letters 392: 49–53.

Nakane K, Tsuchihashi Y, Matsuura N (2013). A simple mathematical model utilizing topological invariants for automatic detection of tumor areas in digital tissue images. Diagnostic Pathology 8: 1–4.

Nichols SM, Bavister BD, Brenner CA, Didier PJ, Harrison RM, Kubisch HM (2005). Ovarian senescence in the rhesus monkey (*Macaca mulatta*). Human Reproduction, 20(1), 79–83.

Nozaki M, Mitsunaga F, Shimizu K (1995). Reproductive senescence in female Japanese monkeys (Macaca fuscata): age- and season-related changes in hypothalamic-pituitary-ovarian functions and fecundity rates. Biology of Reproduction 52: 1250–1257.

Onouchi T, Kato J (1983). Estrogen receptors and estrogen-inducible progestin receptors in the sexual skin of the monkey. Journal of Steroid Biochemistry 18: 145–151.

Ozasa H, Gould KG (1982). Demonstration and Characterization of Estrogen Receptor in Chimpanzee Sex Skin: Correlation between Nuclear Receptor Levels and Degree of Swelling. Endocrinology 111: 125-131

Pathak MA, Riley FJ, Fitzpatrick TB, Curwen WL (1962). Melanin formation in human skin induced by long-wave ultra-violet and visible light. Nature 193: 148–150.

Pelletier G (2000). Localization of androgen and estrogen receptors in rat and primate tissues. Histology and Histopathology 15: 1261–1270.

Ranson M, Posen S, Mason RS (1988). Human melanocytes as a target tissue for hormones: in vitro studies with 1 alpha-25, dihydroxyvitamin D3,

alpha-melanocyte stimulating hormone, and beta-estradiol. Journal of Investigative Dermatology 91: 593–598.

Renoult JP, Schaefer HM, Sallé B, Charpentier MJE (2011). The evolution of the multicoloured face of mandrills: insights from the perceptual space of colour vision. PLOS ONE 6: e29117.

Saidi IS, Jacques SL, Tittel FK (1995). Mie and Rayleigh modeling of visible-light scattering in neonatal skin. Applied Optics 34: 7410–7418.

Setchell JM, Wickings EJ (2004). Sexual swelling in mandrills (Mandrillus sphinx): a test of the reliable indicator hypothesis. Behavioral Ecology 15: 438–445.

Sobel H, Lee KD, Hewlett MJ (1965). Effect of estrogen on acid glycosaminoglycans in skin of mice. Biochimica et Biophysica Acta (BBA) - Mucoproteins and Mucopolysaccharides 101: 225–229.

Stegmann TJ (1998). FGF-1: a human growth factor in the induction of neoangiogenesis. Expert Opinion on Investigational Drugs 7: 2011–2015.

Stephen ID, Law Smith MJ, Stirrat MR, Perrett DI (2009). Facial skin coloration affects perceived health of human faces. International Journal of Primatology 30: 845–857.

Stevens M, Stoddard MC, Higham JP (2009). Studying primate color: towards visual system-dependent methods. International Journal of Primatology 30: 893–917.

Takahashi N, Tonchev AB, Koike K, Murakami K, Yamada K, Yamashima T, Inoue M (2004). Expression of estrogen receptor-β in the postischemic monkey hippocampus. Neuroscience Letters 369: 9–13.

Takahata Y, Koyama N, Suzuki S (1995). Do the old aged females experience a long post-reproductive life span?: The cases of Japanese macaques and chimpanzees. Primates 36: 169-180.

Takiwaki H (1998). Measurement of skin color: practical application and theoretical considerations. The Journal of Medical Investigation 44: 121–126.

Thierry B (2010). The macaques - a double-layered social organization. In: Primates in Perspective, 2nd ed. (Campbell C, Fuentes A, MacKinnon K, Bearder S, Stumpf R, eds.), pp 229–241. Oxford University Press.

Thornton MJ (2002). The biological actions of estrogens on skin. Experimental Dermatology 11: 487–502.

Tosi AJ, Morales JC, Melnick DJ (2000). Comparison of Y chromosome and mtDNA phylogenies leads to unique inferences of macaque evolutionary history. Molecular Phylogenetics and Evolution 17: 133–44.

Vorobyev M, Osorio D (1998). Receptor noise as a determinant of colour thresholds. Proceedings of the Royal Society B: Biological Sciences 265: 351–8.

Waitt C, Gerald MS, Little AC, Kraiselburd E (2006). Selective attention toward female secondary sexual color in male rhesus macaques. American Journal of Primatology 68: 738–744.

Walker ML (1995). Menopause in female rhesus monkeys. American Journal of Primatology, 35(1), 59–71.

Wallner B, Aspernig D, Millesi E, Machatschke IH (2011). Non-lactating versus lactating females: a comparison of sex steroids, sexual coloration, and sexual

behavior in Japanese macaques. Primates 52: 69–75.

Watson KK, Ghodasra JH, Furlong MA, Platt ML (2012). Visual preferences for sex and status in female rhesus macaques. Animal Cognition 15: 401–407.

Weatherall IL, Coombs BD (1992). Skin color measurements in terms of CIELAB color space values. Journal of Investigative Dermatology 99: 468–473.

Wickler W (1967). Socio-sexual signals and their intra-specific imitation among primates. In Primate Ethology (Morris D eds.), pp 69–147. London, Weidenfeld and Nicolson.

Wildt DE, Doyle LL, Stone SC, Harrison RM (1977). Correlation of perineal swelling with serum ovarian hormone levels, vaginal cytology, and ovarian follicular development during the baboon reproductive cycle. Primates 18:261–270.

Young C, Majolo B, Heistermann M, Schülke O, Ostner J (2013). Male mating behaviour in relation to female sexual swellings, socio-sexual behaviour and hormonal changes in wild Barbary macaques. Hormones and Behavior 63:32–9.

Zonios G, Bykowski J, Kollias N (2001). Skin melanin, hemoglobin, and light scattering properties can be quantitatively assessed in vivo using diffuse reflectance spectroscopy. Journal of Investigative Dermatology 117: 1452–1457.